

FIG. 4. Molecular interactions of GRL-02031 with HIV-1 protease. (A) A model of the interaction of GRL-02031 with HIV protease. The bird's-eye view of the docked pose (inset) is presented along with a blown-up figure highlighting the important hydrogen bond interactions. The inhibitor is predicted to have hydrogen bond interactions with Asp25, Gly27, Asp29, Ile50, Asp29', and Ile50'. Note that the pyrrolidone oxygen (red stick) interacts with the S-2' subpocket and forms a hydrogen bond interaction with Asp29'. (B) Superimposed binding configurations of GRL-02031 with the HIV-1 protease. The carbons are shown in gray in configuration 1 and in green in configuration 2. Selected hydrogen bond interactions of configuration 2 are shown. In configuration 2, the methoxybenzene interacts with the S-2' site and forms a hydrogen bond interaction with Asp30'. The interaction of the P-2 ligand Cp-THF is the same in both configurations. (C) The binding cavity of HIV protease with lipophilic potential is shown. GRL-02031 fits tightly in the binding cavity and has favorable polar and nonpolar interactions with the active-site residues of the HIV-1 protease. The van der Waals surfaces of Ile47 and Ile47' (both in magenta) and of Ile84' (in purple) demonstrate that they form tight nonpolar interactions with GRL-02031. The protease residues are shown in stick representation. The following atoms are indicated by designated colors: C, gray; O, red; N, blue; S, yellow; H, cyan. Both protease chains are shown in green. The figure was generated with the MOLCAD program (Sybyl, version 8.0; Tripos, L.P., St. Louis, MO).

seen in the case of DRV (9). This resistance profile (i.e., the requirement of multiple mutations) of GRL-02031 may also confer certain advantage in the resistance profile of GRL-02031.

Two mutations at conserved residues, L33F and Q58E, also emerged by passage 37 and were present in 10 and 9 of 10 clones, respectively. L33F has primarily been reported in patients treated with RTV or APV (37). The L33F substitution alone did not change the susceptibility of HIV-1 to GRL-02031 (Table 4), although it has recently gained attention because of its association with resistance to the FDA-approved PI, tipranavir (33).

In the HIV-1 variants selected with GRL-02031, four amino acid substitutions in the Gag proteins (G62R, R409K, L363M, and I437T) were seen by passage 37. R409K within the p7 Gag seems to be associated with viral resistance to APV (14), although the significance of G62R within p17 is as yet unknown. The p7-p1 cleavage-site mutation I437T has been reported to be associated with ATV resistance (17). It is of note that by passage 15, an unusual amino acid substitution, L363M, emerged; this substitution has not previously been reported in relation to PI resistance. This L363M is located at the p24-p2 cleavage site, which represents the C terminus of the capsid (CA) p24 protein that is highly conserved and that is involved

in virion assembly. The deletion of this cluster or the introduction of mutations such as L363A is known to cause significant impairment of particle formation and infectivity (34). It is noteworthy that L363M appears in HIV-1 variants resistant to a maturation inhibitor, PA-457 [3-O-(3',3'-dimethylsuccinyl) betulonic acid], which binds to the CA-p2 cleavage site or its proximity, blocks the cleavage by protease during virion maturation, and exerts activity against HIV-1 (27, 44, 49).

It was noted that GRL-02031 and SQV remained active against most of the PI-selected HIV-1 variants and that SQV, IDV, and NFV remained potent against HIV-1_{GRL-02031-5} μM (Table 3), suggesting that the combination of GRL-02031, SQV, IDV, and NFV can exert complementarily augmented activity against multi-PI-resistant HIV-1 variants. Such a difference in the resistance profile of GRL-02031 when it is used with SQV and NFV may be due to the differences in binding and antiviral potency associated with the D30N and G48V mutations (Table 4).

In an attempt to explain why GRL-02031 can exert potent activity against a wide spectrum of HIV-1 variants resistant to multiple PIs, we performed structural modeling and molecular docking of the interactions of GRL-02031 with protease (Fig. 4). Interestingly, our structural modeling analysis demonstrated that there are two distinct binding modes of GRL-

02031 in the S-2' pocket of the protease. Either the 2-pyrrolidone group or the methoxybenzene moiety can orient toward Asp29' and Asp30' (configuration 1 and configuration 2, respectively) (Fig. 4B). It is presumed that such alternate binding modes provide distinct advantages to GRL-02031 in maintaining its antiviral activity against a wide spectrum of HIV-1 variants resistant to other currently available PIs. The alternate binding modes could explain the reason why the development of resistance to GRL-02031 is substantially delayed compared to the time to the development of resistance to APV or IDV (Fig. 2). In addition, the models of GRL-02031 indicated that it is capable of forming hydrogen bond interactions with the backbone atoms of Asp29, Asp29', and/or Asp30'. Such backbone interactions have been shown to be important in maintaining potency not only against wild-type protease but also against drug-resistant mutant proteases (1, 15, 16, 36). This may also explain why GRL-02031 maintains its potency against a wide variety of drug-resistant mutant proteases.

It is of note that the difference seen with GRL-02031 (one- to twofold) seems substantially less than that seen with DRV (one- to sevenfold) (Table 2). Although this difference may not be translated into an actual difference in the clinical setting, it is worth noting that GRL-02031 may have certain advantages in its activity against highly drug-resistant HIV-1 variants. Considering that the acquisition of multiple amino acid substitutions is required for the emergence of HIV-1 resistance to GRL-02031, the profile of HIV-1 resistance to GRL-02031, which is apparently different from the profiles for the other PIs, might result in an advantage for GRL-02031, although further evaluations, including testing of the compound in the clinical setting, are required.

Taken together, GRL-02031 exerts potent activity against a wide spectrum of laboratory and clinical wild-type and multi-drug-resistant HIV-1 strains without significant cytotoxicity in vitro and substantially delays the emergence of HIV-1 variants resistant to GRL-02031. These data warrant further consideration of GRL-02031 as a candidate as a novel PI for the treatment of AIDS.

ACKNOWLEDGMENTS

We thank Shintaro Matsumi, Toshikazu Miyakawa, and Manabu Aoki for helpful discussion.

This work was supported in part by the Intramural Research Program of the Center for Cancer Research, National Cancer Institute, National Institutes of Health (to D.D., H.N., and H.M.); a grant from the National Institutes of Health (grant GM 53386 to A.K.G.); a grant from a Research for the Future Program of the Japan Society for the Promotion of Science (grant JSPS-RFTF 97L00705 to H.M.); a Grant-in-Aid for Scientific Research (grant for priority areas to H.M.) from the Ministry of Education, Culture, Sports, Science, and Technology (Monbu-Kagakusho) of Japan; and a Grant for Promotion of AIDS Research from the Ministry of Health, Labor and Welfare (Kosei-Rodosho) of Japan (to H.M.).

This work utilized the computational resources of the Biowulf cluster at the NIH.

REFERENCES

- Amano, M., Y. Koh, D. Das, J. Li, S. Leschenko, Y. F. Wang, P. I. Boross, I. T. Weber, A. K. Ghosh, and H. Mitsuya. 2007. A novel bis-tetrahydrofuran-ylurethane-containing nonpeptidic protease inhibitor (PI), GRL-98065, is potent against multiple-PI-resistant human immunodeficiency virus in vitro. *Antimicrob. Agents Chemother.* 51:2143-2155.
- Antiretroviral Therapy Cohort Collaboration. 2008. Life expectancy of individuals on combination antiretroviral therapy in high-income countries: a collaborative analysis of 14 cohort studies. *Lancet* 372:293-299.
- Bhaskaran, K., O. Hamouda, M. Sannes, F. Boufassa, A. M. Johnson, P. C. Lambert, and K. Porter. 2008. Changes in the risk of death after HIV seroconversion compared with mortality in the general population. *JAMA* 300:51-59.
- Cho, A. E., V. Guallar, B. J. Berne, and R. Friesner. 2005. Importance of accurate charges in molecular docking: quantum mechanical/molecular mechanical (QM/MM) approach. *J. Comput. Chem.* 26:915-931.
- Clotet, B., N. Bellos, J. M. Molina, D. Cooper, J. C. Goffard, A. Lazzarin, A. Wöhrmann, C. Katlama, T. Wilkin, R. Haubrich, C. Cohen, C. Farthing, D. Jayaweera, M. Markowitz, P. Ruane, S. Spinosa-Guzman, and E. Lefebvre. 2007. Efficacy and safety of darunavir-ritonavir at week 48 in treatment-experienced patients with HIV-1 infection in POWER 1 and 2: a pooled subgroup analysis of data from two randomised trials. *Lancet* 369:1169-1178.
- Condra, J. H., W. A. Schleif, O. M. Blahy, L. J. Gabryelski, D. J. Graham, J. C. Quintero, A. Rhodes, H. L. Robbins, E. Roth, M. Shivaprakash, et al. 1995. In vivo emergence of HIV-1 variants resistant to multiple protease inhibitors. *Nature* 374:569-571.
- De Clercq, E. 2002. Strategies in the design of antiviral drugs. *Nat. Rev. Drug Discov.* 1:13-25.
- de Mendoza, C., and V. Soriano. 2004. Resistance to HIV protease inhibitors: mechanisms and clinical consequences. *Curr. Drug Metab.* 5:321-328.
- De Meyer, S., H. Azijn, D. Surleraux, D. Jochmans, A. Tahrir, R. Pauwels, P. Wigerinck, and M. P. de Bethune. 2005. TMC114, a novel human immunodeficiency virus type 1 protease inhibitor active against protease inhibitor-resistant viruses, including a broad range of clinical isolates. *Antimicrob. Agents Chemother.* 49:2314-2321.
- Erickson, J. W., and S. K. Burt. 1996. Structural mechanisms of HIV drug resistance. *Annu. Rev. Pharmacol. Toxicol.* 36:545-571.
- Ferrer, E., D. Podzameczer, M. Arnedo, E. Fumero, P. McKenna, A. Rinehart, J. L. Perez, M. J. Barbera, T. Pumarola, J. M. Gatell, and F. Gudiol. 2003. Genotype and phenotype at baseline and at failure in human immunodeficiency virus-infected antiretroviral-naive patients in a randomized trial comparing zidovudine and lamivudine plus nelfinavir or nevirapine. *J. Infect. Dis.* 187:687-690.
- Friesner, R. A., J. L. Banks, R. B. Murphy, T. A. Halgren, J. J. Klicic, D. T. Mainz, M. P. Repasky, E. H. Knoll, M. Shelley, J. K. Perry, D. E. Shaw, P. Francis, and P. S. Shenkin. 2004. Glide: a new approach for rapid, accurate docking and scoring. 1. Method and assessment of docking accuracy. *J. Med. Chem.* 47:1739-1749.
- Friesner, R. A., R. B. Murphy, M. P. Repasky, L. L. Frye, J. R. Greenwood, T. A. Halgren, P. C. Sanschagrin, and D. T. Mainz. 2006. Extra precision glide: docking and scoring incorporating a model of hydrophobic enclosure for protein-ligand complexes. *J. Med. Chem.* 49:6177-6196.
- Gatanaga, H., Y. Suzuki, H. Tsang, K. Yoshimura, M. F. Kavlick, K. Nagashima, R. J. Gorelick, S. Mardy, C. Tang, M. F. Summers, and H. Mitsuya. 2002. Amino acid substitutions in Gag protein at non-cleavage sites are indispensable for the development of a high multitude of HIV-1 resistance against protease inhibitors. *J. Biol. Chem.* 277:5952-5961.
- Ghosh, A. K., B. D. Chapsal, I. T. Weber, and H. Mitsuya. 2008. Design of HIV protease inhibitors targeting protein backbone: an effective strategy for combating drug resistance. *Acc. Chem. Res.* 41:78-86.
- Ghosh, A. K., P. R. Sridhar, S. Leshchenko, A. K. Hussain, J. Li, A. Y. Kovalevsky, D. E. Walters, J. E. Wedekind, V. Grum-Tokars, D. Das, Y. Koh, K. Maeda, H. Gatanaga, I. T. Weber, and H. Mitsuya. 2006. Structure-based design of novel HIV-1 protease inhibitors to combat drug resistance. *J. Med. Chem.* 49:5252-5261.
- Gong, Y. F., B. S. Robinson, R. E. Rose, C. Deminie, T. P. Spicer, D. Stock, R. J. Colonna, and P. F. Lin. 2000. In vitro resistance profile of the human immunodeficiency virus type 1 protease inhibitor BMS-232632. *Antimicrob. Agents Chemother.* 44:2319-2326.
- Gupta, R., A. Hill, A. W. Sawyer, and D. Pillay. 2008. Emergence of drug resistance in HIV type 1-infected patients after receipt of first-line highly active antiretroviral therapy: a systematic review of clinical trials. *Clin. Infect. Dis.* 47:712-722.
- Hertogs, K., S. Bloor, S. D. Kemp, C. Van den Eynde, T. M. Alcorn, R. Pauwels, M. Van Houtte, S. Staszewski, V. Miller, and B. A. Larder. 2000. Phenotypic and genotypic analysis of clinical HIV-1 isolates reveals extensive protease inhibitor cross-resistance: a survey of over 6000 samples. *AIDS* 14:1203-1210.
- Hicks, C. B., P. Cahn, D. A. Cooper, S. L. Walmsley, C. Katlama, B. Clotet, A. Lazzarin, M. A. Johnson, D. Neubacher, D. Mayers, and H. Valdez. 2006. Durable efficacy of tipranavir-ritonavir in combination with an optimised background regimen of antiretroviral drugs for treatment-experienced HIV-1-infected patients at 48 weeks in the Randomized Evaluation of Strategic Intervention in multi-drug resistant patients with Tipranavir (RESIST) studies: an analysis of combined data from two randomised open-label trials. *Lancet* 368:466-475.
- Jacobsen, H., K. Yasargil, D. L. Winslow, J. C. Craig, A. Krohn, I. B. Duncan, and J. Mous. 1995. Characterization of human immunodeficiency virus type 1 mutants with decreased sensitivity to proteinase inhibitor Ro 31-8959. *Virology* 206:527-534.
- Kantor, R., W. J. Fessel, A. R. Zolopa, D. Israelski, N. Shulman, J. G.

- Montoya, M. Harbour, J. M. Schapiro, and R. W. Shafer. 2002. Evolution of primary protease inhibitor resistance mutations during protease inhibitor salvage therapy. *Antimicrob. Agents Chemother.* **46**:1086–1092.
23. Kaplan, A. H., S. F. Michael, R. S. Webbie, M. F. Knigge, D. A. Paul, L. Everitt, D. J. Kempf, D. W. Norbeck, J. W. Erickson, and R. Swanstrom. 1994. Selection of multiple human immunodeficiency virus type 1 variants that encode viral proteases with decreased sensitivity to an inhibitor of the viral protease. *Proc. Natl. Acad. Sci. USA* **91**:5597–5601.
 24. Kemper, C. A., M. D. Witt, P. H. Keiser, M. P. Dube, D. N. Forthal, M. Leibowitz, D. S. Smith, A. Rigby, N. S. Hellmann, Y. S. Lie, J. Leedom, D. Richman, J. A. McCutchan, and R. Haubrich. 2001. Sequencing of protease inhibitor therapy: insights from an analysis of HIV phenotypic resistance in patients failing protease inhibitors. *AIDS* **15**:609–615.
 25. Koh, Y., S. Matsumi, D. Das, M. Amano, D. A. Davis, J. Li, S. Leschenko, A. Baldrige, T. Shioda, R. Yarchoan, A. K. Ghosh, and H. Mitsuya. 2007. Potent inhibition of HIV-1 replication by novel non-peptidyl small molecule inhibitors of protease dimerization. *J. Biol. Chem.* **282**:28709–28720.
 26. Koh, Y., H. Nakata, K. Maeda, H. Ogata, G. Bilcer, T. Devasamudram, J. F. Kincaid, P. Boross, Y. F. Wang, Y. Tie, P. Volarath, L. Gaddis, R. W. Harrison, I. T. Weber, A. K. Ghosh, and H. Mitsuya. 2003. Novel bis-tetrahydrofuranyurethane-containing nonpeptidic protease inhibitor (PI) UIC-94017 (TMC114) with potent activity against multi-PI-resistant human immunodeficiency virus in vitro. *Antimicrob. Agents Chemother.* **47**:3123–3129.
 27. Li, F., R. Goila-Gaur, K. Salzwedel, N. R. Kilgore, M. Reddick, C. Matallana, A. Castillo, D. Zoumplis, D. E. Martin, J. M. Orenstein, G. P. Allaway, E. O. Freed, and C. T. Wild. 2003. PA-457: a potent HIV inhibitor that disrupts core condensation by targeting a late step in Gag processing. *Proc. Natl. Acad. Sci. USA* **100**:13555–13560.
 28. Little, S. J., S. Holte, J. P. Routy, E. S. Daar, M. Markowitz, A. C. Collier, R. A. Koup, J. W. Mellors, E. Connick, B. Conway, M. Kilby, L. Wang, J. M. Whitcomb, N. S. Hellmann, and D. D. Richman. 2002. Antiretroviral-drug resistance among patients recently infected with HIV. *N. Engl. J. Med.* **347**:385–394.
 29. Maeda, K., H. Nakata, Y. Koh, T. Miyakawa, H. Ogata, Y. Takaoka, S. Shibayama, K. Sagawa, D. Fukushima, J. Moravek, Y. Koyanagi, and H. Mitsuya. 2004. Spirodiketopiperazine-based CCR5 inhibitor which preserves CC-chemokine/CCR5 interactions and exerts potent activity against R5 human immunodeficiency virus type 1 in vitro. *J. Virol.* **78**:8654–8662.
 30. Maeda, K., K. Yoshimura, S. Shibayama, H. Habashita, H. Tada, K. Sagawa, T. Miyakawa, M. Aoki, D. Fukushima, and H. Mitsuya. 2001. Novel low molecular weight spirodiketopiperazine derivatives potently inhibit R5 HIV-1 infection through their antagonistic effects on CCR5. *J. Biol. Chem.* **276**:35194–35200.
 31. Maguire, M., D. Shortino, A. Klein, W. Harris, V. Manohitharajah, M. Tisdale, R. Elston, J. Yeo, S. Randall, F. Xu, H. Parker, J. May, and W. Snowden. 2002. Emergence of resistance to protease inhibitor amprenavir in human immunodeficiency virus type 1-infected patients: selection of four alternative viral protease genotypes and influence of viral susceptibility to coadministered reverse transcriptase nucleoside inhibitors. *Antimicrob. Agents Chemother.* **46**:731–738.
 32. Mammano, F., V. Trouplin, V. Zennou, and F. Clavel. 2000. Retracing the evolutionary pathways of human immunodeficiency virus type 1 resistance to protease inhibitors: virus fitness in the absence and in the presence of drug. *J. Virol.* **74**:8524–8531.
 33. McCallister, S., V. Kohlbrenner, K. Squires, A. Lazzarin, P. Kumar, E. DeJesus, J. Nadler, J. Gallant, S. Walmsley, P. Yeni, J. Leith, C. Dohnanyi, D. Hall, J. Sabo, T. MacGregor, W. Verbiest, P. McKenna, and D. Mayers. 2003. Characterization of the impact of genotype, phenotype, and inhibitory quotient on antiviral activity of tipranavir in highly treatment-experienced patients. *Antivir. Ther.* **8**:S15.
 34. Melamed, D., M. Mark-Danieli, M. Kenan-Eichler, O. Kraus, A. Castiel, N. Laham, T. Pupko, F. Glaser, N. Ben-Tal, and E. Bacharach. 2004. The conserved carboxy terminus of the capsid domain of human immunodeficiency virus type 1 Gag protein is important for virion assembly and release. *J. Virol.* **78**:9675–9688.
 35. Mitsuya, H., and J. Erickson. 1999. Discovery and development of antiretroviral therapeutics for HIV infection, p. 751–780. *In* T. C. Merigan, J. G. Bartlett, and D. Bolognesi (ed.), *Textbook of AIDS medicine*. The Williams & Wilkins Co., Baltimore, MD.
 36. Mitsuya, H., K. Maeda, D. Das, and A. K. Ghosh. 2008. Development of protease inhibitors and the fight with drug-resistant HIV-1 variants. *Adv. Pharmacol.* **56**:169–197.
 37. Molla, A., M. Korneyeva, Q. Gao, S. Vasavanonda, P. J. Schipper, H. M. Mo, M. Markowitz, T. Chernyavskiy, P. Niu, N. Lyons, A. Hsu, G. R. Granneman, D. D. Ho, C. A. Boucher, J. M. Leonard, D. W. Norbeck, and D. J. Kempf. 1996. Ordered accumulation of mutations in HIV protease confers resistance to ritonavir. *Nat. Med.* **2**:760–766.
 38. Murphy, E. L., A. C. Collier, L. A. Kalish, S. F. Assmann, M. F. Para, T. P. Flanigan, P. N. Kumar, L. Mintz, F. R. Wallach, and G. J. Nemo. 2001. Highly active antiretroviral therapy decreases mortality and morbidity in patients with advanced HIV disease. *Ann. Intern. Med.* **135**:17–26.
 39. Murphy, R. L. 2000. New antiretroviral drugs in development. *AIDS* **14**(Suppl. 3):S227–S234.
 40. Partaledis, J. A., K. Yamaguchi, M. Tisdale, E. E. Blair, C. Falcione, B. Maschera, R. E. Myers, S. Pazhanisamy, O. Futer, A. B. Cullinan, C. M. Stuver, R. A. Byrn, and D. J. Livingston. 1995. In vitro selection and characterization of human immunodeficiency virus type 1 (HIV-1) isolates with reduced sensitivity to hydroxyethylamino sulfonamide inhibitors of HIV-1 aspartyl protease. *J. Virol.* **69**:5228–5235.
 41. Patick, A. K., M. Duran, Y. Cao, D. Shugarts, M. R. Keller, E. Mazabel, M. Knowles, S. Chapman, D. R. Kuritzkes, and M. Markowitz. 1998. Genotypic and phenotypic characterization of human immunodeficiency virus type 1 variants isolated from patients treated with the protease inhibitor nelfinavir. *Antimicrob. Agents Chemother.* **42**:2637–2644.
 42. Prado, J. G., T. Wrin, J. Beauchaine, L. Ruiz, C. J. Petropoulos, S. D. Frost, B. Clotet, R. T. D'Aquila, and J. Martinez-Picado. 2002. Amprenavir-resistant HIV-1 exhibits lopinavir cross-resistance and reduced replication capacity. *AIDS* **16**:1009–1017.
 43. Rodriguez-Barrios, F., and F. Gago. 2004. HIV protease inhibition: limited recent progress and advances in understanding current pitfalls. *Curr. Top. Med. Chem.* **4**:991–1007.
 44. Salzwedel, K., R. Goila-Gaur, C. Adamson, F. Li, A. Castillo, N. Kilgore, M. Reddick, C. Matallana, D. Zoumplis, D. Martin, G. Allaway, E. Freed, and C. Wild. 2004. Selection for and characterization of HIV-1 isolates resistant to the maturation inhibitor PA-457. *Antivir. Ther.* **9**:S8.
 45. Shirasaka, T., M. F. Kavlick, T. Ueno, W. Y. Gao, E. Kojima, M. L. Alcaide, S. Chokekijchai, B. M. Roy, E. Arnold, R. Yarchoan, et al. 1995. Emergence of human immunodeficiency virus type 1 variants with resistance to multiple dideoxynucleosides in patients receiving therapy with dideoxynucleosides. *Proc. Natl. Acad. Sci. USA* **92**:2398–23402.
 46. Walensky, R. P., A. D. Paltiel, E. Losina, L. M. Mercincavage, B. R. Schackman, P. E. Sax, M. C. Weinstein, and K. A. Freedberg. 2006. The survival benefits of AIDS treatment in the United States. *J. Infect. Dis.* **194**:11–19.
 47. Yoshimura, K., R. Kato, M. F. Kavlick, A. Nguyen, V. Maroun, K. Maeda, K. A. Hussain, A. K. Ghosh, S. V. Gulnik, J. W. Erickson, and H. Mitsuya. 2002. A potent human immunodeficiency virus type 1 protease inhibitor, UIC-94003 (TMC-126), and selection of a novel (A28S) mutation in the protease active site. *J. Virol.* **76**:1349–1358.
 48. Yoshimura, K., R. Kato, K. Yusa, M. F. Kavlick, V. Maroun, A. Nguyen, T. Mimoto, T. Ueno, M. Shintani, J. Falloun, H. Masur, H. Hayashi, J. Erickson, and H. Mitsuya. 1999. JE-2147: a dipeptide protease inhibitor (PI) that potently inhibits multi-PI-resistant HIV-1. *Proc. Natl. Acad. Sci. USA* **96**:8675–8680.
 49. Zhou, J., X. Yuan, D. Dismuke, B. M. Forshey, C. Lundquist, K. H. Lee, C. Aiken, and C. H. Chen. 2004. Small-molecule inhibition of human immunodeficiency virus type 1 replication by specific targeting of the final step of virion maturation. *J. Virol.* **78**:922–929.

Design and Synthesis of Stereochemically Defined Novel Spirocyclic P2-Ligands for HIV-1 Protease Inhibitors

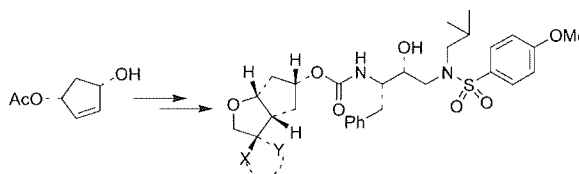
Arun K. Ghosh,^{*,†} Bruno D. Chapsal,[†] Abigail Baldrige,[†] Kazuhiko Ide,[‡] Yashiro Koh,[‡] and Hiroaki Mitsuya^{‡,§}

Departments of Chemistry and Medicinal Chemistry, Purdue University, West Lafayette, Indiana 47907, Department of Hematology and Infectious Diseases, Kumamoto University School of Medicine, Kumamoto 860-8556, Japan, and Experimental Retrovirology Section, HIV and AIDS Malignancy Branch, Center for Cancer Research, National Cancer Institute, Bethesda, Maryland 20892

akghosh@purdue.edu

Received August 29, 2008

ABSTRACT



The synthesis of a series of stereochemically defined spirocyclic compounds and their use as novel P2-ligands for HIV-1 protease inhibitors are described. The bicyclic core of the ligands was synthesized by an efficient *n*Bu₃SnH-promoted radical cyclization of a 1,6-enyne followed by oxidative cleavage. Structure-based design, synthesis of ligands, and biological evaluations of the resulting inhibitors are reported.

The introduction of highly active antiretroviral therapy (HAART) in 1996, in combination with HIV-1 protease inhibitors and reverse transcriptase inhibitors, has dramatically changed the management of HIV/AIDS.¹ The advent of HAART has significantly reduced morbidity and mortality and has improved the quality of life for HIV-infected patients, particularly in developed nations.² Despite this important breakthrough, current and future management of HIV/AIDS is being challenged by the rapid emergence of multi-drug-resistant HIV-1 strains and drug-related side effects.³ Consequently, development of novel and effective treatment regimens are critically important.

In our continuing effort to design a new generation of HIV-1 protease inhibitors (PIs) that combat drug resistance, we developed a series of exceedingly potent PIs. A number of these nonpeptidyl PIs have shown superb antiviral activity and drug-resistance profiles. In our structure-based design strategies, we introduced the “backbone binding concept” with the presumption that an inhibitor that makes maximum interactions in the protease active site, particularly hydrogen bonding with the backbone atoms, may retain its potency against mutant strains.⁴ Darunavir (**1**, Figure 1), which has been approved by the FDA for the treatment of patients harboring multi-drug-resistant HIV-1 strains, has emerged from this approach.^{5,6} Our detailed X-ray structural analysis of protein–ligand complexes revealed an extensive hydrogen

[†] Purdue University.

[‡] Kumamoto University School of Medicine.

[§] National Cancer Institute.

(1) Sepkowitz, K. A. *N. Engl. J. Med.* **2001**, *344*, 1764.

(2) Palella, F. J.; Delaney, K. M.; Moorman, A. C.; Loveless, M. O.; Fuhrer, J.; Satten, G. A.; Aschman, D. J.; Homborg, S. D. *N. Engl. J. Med.* **1998**, *338*, 853.

(3) Boden, D.; Markowitz, M. *Antimicrob. Agents Chemother.* **1998**, *42*, 2775.

(4) Ghosh, A. K.; Chapsal, B. D.; Weber, I. T.; Mitsuya, H. *Acc. Chem. Res.* **2008**, *41*, 78.

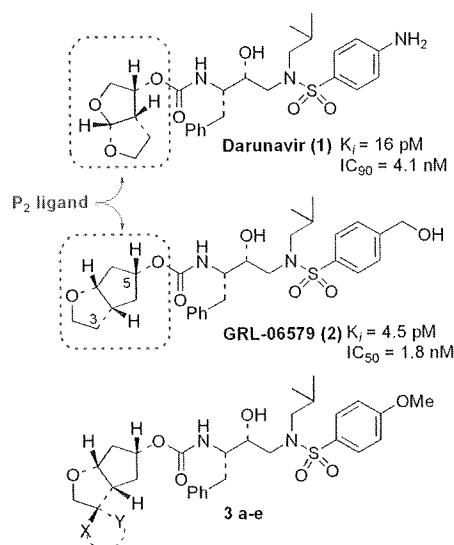


Figure 1. Structure of HIV protease inhibitors.

bonding network with HIV-1 protease backbone atoms and most notably with the designed bis-THF P2-ligand.⁷

More recently, we reported another novel PI, GRL-06579 (**2**), which features a stereochemically defined bicyclic hexahydrocyclopentylfuran (Cp-THF) P2-ligand in the hydroxyethylsulfonamide isostere core.⁸ The X-ray crystallographic analysis of **2**-bound HIV-1 protease documented extensive hydrogen bonding interactions including the Cp-THF oxygen with the backbone atoms in the S2-subsite.⁸

The favorable drug-resistance profile of this PI containing the Cp-THF ligand logically prompted us to design several structural analogs. We set out to introduce new functionalities on this bicyclic core that could create additional interactions within the enzyme catalytic site. The 3-position of the Cp-THF ligand appeared particularly suitable for this purpose, because of its proximity to the flap region and the S2-subsite of the protease. Based upon our analysis of the X-ray crystal structure of **2**-bound protease, we planned to investigate the effect of a structurally constrained spirocyclic motif at the 3-position of the Cp-THF ring. We speculated that a cyclic ether oxygen or an oxazolidinone carbonyl oxygen may be positioned in this cyclic motif to accept a hydrogen bond from the enzyme active site residues or a backbone NH. Such a functionality would fill in the hydrophobic pocket in the S2-subsite as well. Furthermore, this structural feature may improve the pharmacological profile of these inhibitors.^{9,10}

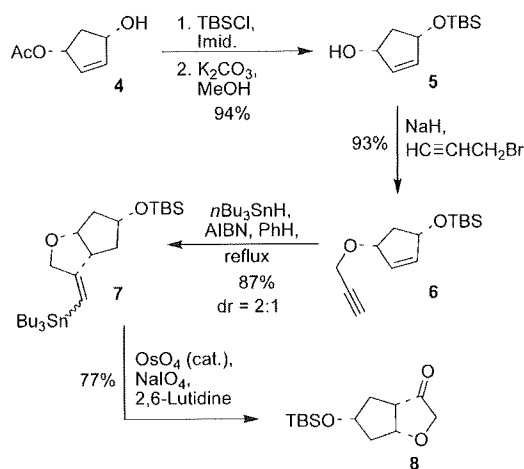
(5) Ghosh, A. K.; Kincaid, J. F.; Cho, W.; Walters, D. E.; Krishnan, K.; Hussain, K. A.; Koo, Y.; Cho, H.; Rudall, C.; Holland, L.; Buthod, J. *Bioorg. Med. Chem. Lett.* **1998**, *8*, 687.

(6) Koh, Y.; Nakata, H.; Maeda, K.; Ogata, H.; Bilcer, G.; Devasamudram, T.; Kincaid, J. F.; Boross, P.; Wang, Y.-F.; Tie, Y.; Volarath, P.; Gaddis, L.; Harrison, R. W.; Weber, I. T.; Ghosh, A. K.; Mitsuya, H. *Antimicrob. Agents Chemother.* **2003**, *47*, 3123.

(7) Kovalevsky, A. Y.; Liu, F.; Leshchenko, S.; Ghosh, A. K.; Louis, J. M.; Harrison, R. W.; Weber, I. T. *J. Mol. Biol.* **2006**, *363*, 161.

(8) Ghosh, A. K.; Sridhar, P. R.; Leshchenko, S.; Hussain, A. K.; Li, J.; Kovalevsky, A. Y.; Walters, D. E.; Wedekind, J. E.; Grum-Tokars, V.; Das, D.; Koh, Y.; Maeda, K.; Gatanaga, H.; Weber, I. T.; Mitsuya, H. *J. Med. Chem.* **2006**, *49*, 5252.

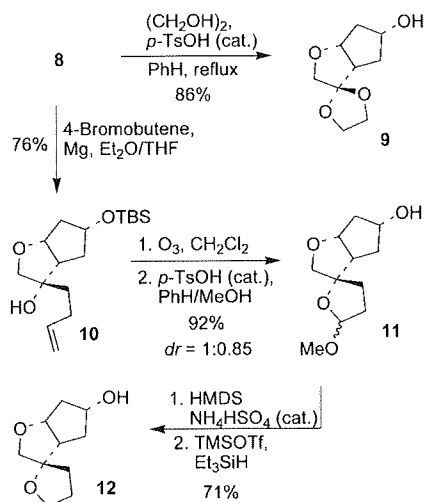
Scheme 1. Synthesis of Bicyclic Ketone **8**



We initially set out to synthesize a series of spirocyclic Cp-THF-derived P2-ligands and their corresponding HIV-protease inhibitors (**3a–e**). A synthetic strategy was devised so that all analogs could be synthesized from a common precursor that gives rapid access to new polycyclic molecular probes. The general synthesis of the bicyclic core of our new P2-ligands was accomplished in enantiomerically pure form as shown in Scheme 1. Optically active monoacetate **4** was obtained in 95% ee by desymmetrization of the corresponding *meso*-diacetate with acetyl cholinesterase.¹¹ Protection of alcohol **4** as a TBS ether followed by methanolysis of the acetyl group furnished compound **5**. Propargylation of **5** using propargyl bromide in the presence of NaH provided alkyne **6** in excellent yield.

The construction of the bicyclic core was accomplished by an intramolecular radical cyclization of alkyne **6** using *n*Bu₃SnH and AIBN in benzene at reflux. This provided vinyl stannane **7** as a mixture of *cis/trans* diastereoisomers (2:1),

Scheme 2. Synthesis of Spirocyclic Ketal and Ether Ligands



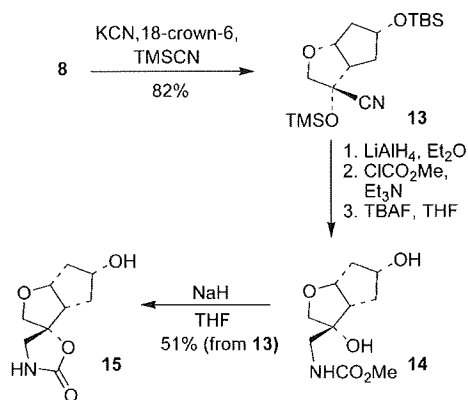
along with trace amounts of the olefin, which presumably formed during purification on silica gel. The mixture of isomers was directly oxidized with a catalytic amount of OsO₄ in the presence of NaIO₄ and 2,6-lutidine to afford the key intermediate, ketone **8** in 77% yield.

We first turned our attention to the synthesis of spirocyclic ketal **9** and ether **12**. Molecular modeling of the corresponding inhibitors suggested that the ligand oxygens could be within hydrogen bonding distance to the NH amide bonds of both Asp30 and Asp29 residues.

Spirocyclic dioxolane ligand **9** was obtained in 86% yield by treatment of ketone **8** with ethylene glycol in benzene with a catalytic amount of *p*-TsOH. Synthesis of ether **12** was achieved in four consecutive steps starting from ketone **8**. Reaction of **8** with homoallyl magnesium bromide furnished compound **10** in 76% yield. Ozonolysis of the terminal alkene and refluxing the resulting crude aldehyde in benzene/methanol followed by azeotropic distillation of the excess methanol afforded methyl acetal **11** as a mixture (1:0.85) of diastereoisomers. Reduction of this acetal intermediate **11** furnished the desired alcohol **12** by applying a one-pot procedure involving (1) TMS-protection of the alcohol with hexamethyldisilazane and (2) subsequent reduction of the acetal with triethylsilane.¹²

We have designed spirocyclic oxazolidinone ligands that could potentially exploit polar interactions with the backbone atoms and residues in the HIV-1 protease active site. Their respective syntheses are highlighted in Scheme 3 and 4.

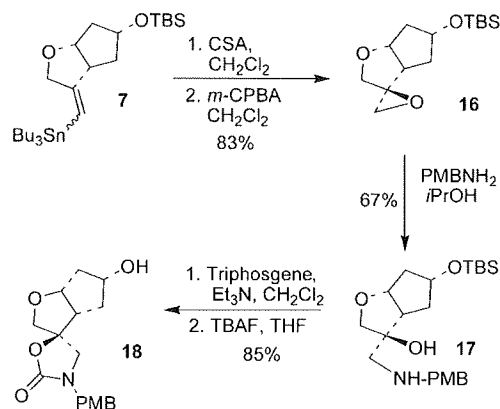
Scheme 3. Synthesis of Spirooxazolidinone Ligand **15**



Cyanohydrin **13** was synthesized in 82% yield from ketone **8**. LiAlH₄-reduction of the cyanide provided the corresponding amine, which exhibited partial TMS-deprotection. Therefore, the crude mixture was directly submitted to the next steps with (1) formation of the methyl carbamate derivative and (2) removal of the silyl ethers with TBAF in THF. The resulting diol **14** was then treated with NaH in THF to give oxazolidinone ligand **15** in 51% yield over four steps (from **13**).

Synthesis of oxazolidinone **18** started with vinylstannane **7** (Scheme 4). Proto-destannylation of **7** was carried out with CSA in CH₂Cl₂. Epoxidation of the resulting olefin with *m*-CPBA gave epoxide **16** as a major diastereomer (93:7 ratio). Opening of the epoxide with *p*-methoxybenzylamine

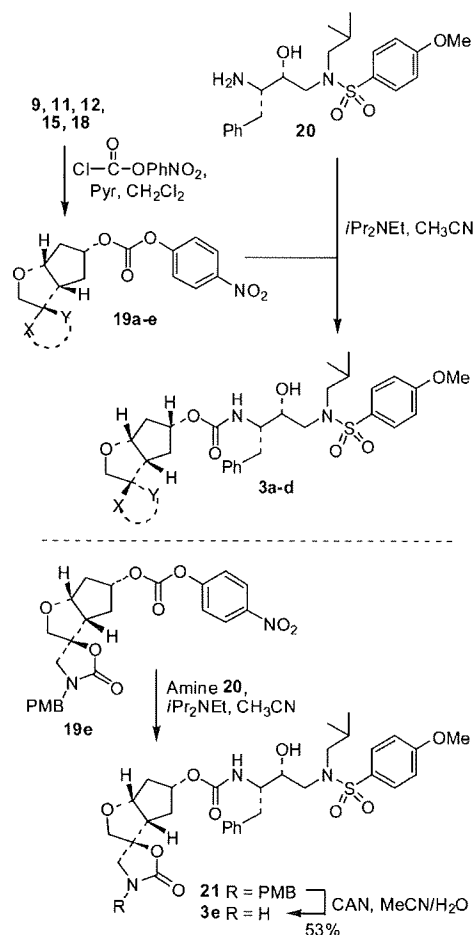
Scheme 4. Synthesis of Spirooxazolidinone Ligand **18**



gave amino alcohol **17** in 67% yield. The carbonyl was installed using triphosgene and Et₃N in CH₂Cl₂. Deprotection of the TBS-group provided the desired oxazolidinone **18**.

The synthesis of polycyclic PIs is shown in Scheme 5. Various synthetic ligands were reacted with 4-nitrophenyl-chloroformate and pyridine to form the corresponding activated carbonates, **19a–e**. Reaction of the respective

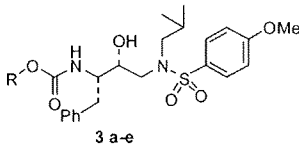
Scheme 5. Synthesis of Inhibitors **3a–e**

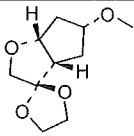
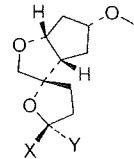
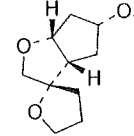
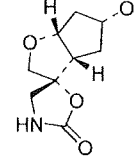
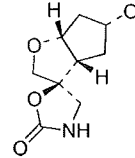


active carbonate with known⁸ amine **20** in the presence of diisopropylethylamine afforded PIs **3a–d**. For the synthesis of inhibitor **3e**, amine **20** was reacted with active carbonate **19e** to provide urethane **21**. Removal of the PMB group from **21** by exposure to ceric ammonium nitrate (CAN) afforded inhibitor **3e**.

We examined all inhibitors for their enzymatic potency as well as their cellular activity, and the results are displayed in Table 1. As shown, most inhibitors exhibited excellent

Table 1. Enzymatic and Antiviral Activity of PIs



Inhibitor	R	K_i (nM) ^a	IC ₅₀ (μM) ^b
3a		0.16	0.28
3b		3b-(S) isomer (X=OMe, Y=H): 0.81	0.23 ^c
		3b-(R) isomer (X=H, Y=OMe): 0.38	
3c		2.22	0.17
3d		0.29	0.093
3e		0.17	0.021

^a K_i determined following protocol as described by Toth and Marshall, mean values of at least four determinations.¹³ ^b MT-2 cells (2×10^4 /mL) were exposed to 100 TCID₅₀ of HIV-1_{LAI} and cultured in the presence of various concentrations of PIs, and the IC₅₀'s were determined by using the MTT assay on day 7 of culture.⁶ ^c Tested as a 1:0.85 mixture.

enzymatic potency. Dioxolane-based analogue **3a** displayed a K_i value of 0.16 nM. Inhibitor **3b** contains the spirocyclic methyl acetal as a mixture (1:0.85 ratio) of diastereomers. These diastereomers were separated by HPLC, and the

stereochemical identity of each diastereomer was determined by extensive NOESY experiments. Diastereomer **3b-(S)** showed an enzymatic K_i of 0.81 nM. The **3b-(R)** isomer is slightly more potent ($K_i = 0.38$ nM). The removal of the methoxy group from **3b** resulted in inhibitor **3c**, which showed a loss of enzyme inhibitory activity. Both inhibitors **3b** and **3c** have shown comparable antiviral activity. We have examined stereochemically defined oxazolidinone derivatives as P2-ligands. Inhibitor **3d** displayed a K_i of 0.29 nM. Diastereomeric inhibitor **3e** is slightly more potent than **3d** in both enzyme inhibitory as well as in antiviral assays (IC₅₀ = 21 nM in MT-2 cells). The inhibitors in Table 1 in general are significantly less potent than UIC-PI (TMC-126),¹⁴ the corresponding methoxysulfonamide derivative of darunavir or Cp-THF-containing inhibitor **2**.⁸

In conclusion we have designed and synthesized a series of inhibitors containing stereochemically defined novel spirocyclic P2-ligands. The syntheses of these ligands were carried out from the key intermediate **8**, which was efficiently prepared in optically active form by using a radical cyclization as the key step. The spirooxazolidinone-derived inhibitor **3e** is the most potent inhibitor in this series. While these inhibitors contain novel P2-ligands, it appears that the spirocyclic motif at the 3-position of the Cp-THF ring resulted in a significant reduction in potency. Further design and optimization of the ligand binding site interactions are in progress.

Acknowledgment. Financial support by the National Institutes of Health (GM 53386, A.K.G.) is gratefully acknowledged. This work was also supported in part by the Intramural Research Program of the Center for Cancer Research, National Cancer Institute, National Institutes of Health, and in part by a Grant-in-aid for Scientific Research (Priority Areas) from the Ministry of Education, Culture, Sports, Science, and Technology of Japan (Monbu Kagakusho) and a Grant for Promotion of AIDS Research from the Ministry of Health, Welfare, and Labor of Japan. We thank Mr. David D. Anderson (Purdue University) for his help with the HPLC and NOESY analysis.

Supporting Information Available: Experimental procedures, spectral data, and ¹H NMR and ¹³C NMR spectra for compounds **5–21** and **3a–e**. This material is available free of charge via the Internet at <http://pubs.acs.org>.

OL8020308

(9) Veber, D. F.; Johnson, S. R.; Cheng, H.-Y.; Smith, B. R.; Ward, K. W.; Kopple, K. D. *J. Med. Chem.* **2002**, *45*, 2615.

(10) Lipinski, C. A. *J. Pharmacol. Toxicol. Methods* **2000**, *44*, 235.

(11) Deardorff, D. R.; Windham, C. Q.; Craney, C. L. *Org. Synth.* **1996**, *9*, 487.

(12) Yoo, S. J.; Kim, H. O.; Lim, Y.; Kim, J.; Jeong, L. S. *Bioorg. Med. Chem.* **2002**, *10*, 215.

(13) Toth, M. V.; Marshall, G. R. *Int. J. Pep. Protein Res.* **1990**, *36*, 544.

(14) Ghosh, A. K.; Sridhar, P.; Kumaragurubaran, N.; Koh, Y.; Weber, I. T.; Mitsuya, H. *ChemMedChem* **2006**, *1*, 937.

Potent HIV-1 protease inhibitors incorporating *meso*-bicyclic urethanes as P2-ligands: structure-based design, synthesis, biological evaluation and protein–ligand X-ray studies†

Arun K. Ghosh,^{*a} Sandra Gemma,^a Jun Takayama,^a Abigail Baldrige,^a Sofiya Leshchenko-Yashchuk,^a Heather B. Miller,^a Yuan-Fang Wang,^b Andrey Y. Kovalevsky,^b Yashiro Koh,^c Irene T. Weber^b and Hiroaki Mitsuya^{c,d}

Received 30th May 2008, Accepted 4th July 2008

First published as an Advance Article on the web 11th August 2008

DOI: 10.1039/b809178a

Recently, we designed a series of novel HIV-1 protease inhibitors incorporating a stereochemically defined bicyclic fused cyclopentyl (Cp-THF) urethane as the high affinity P2-ligand. Inhibitor **1** with this P2-ligand has shown very impressive potency against multi-drug-resistant clinical isolates. Based upon the **1**-bound HIV-1 protease X-ray structure, we have now designed and synthesized a number of *meso*-bicyclic ligands which can conceivably interact similarly to the Cp-THF ligand. The design of *meso*-ligands is quite attractive as they do not contain any stereocenters. Inhibitors incorporating urethanes of bicyclic-1,3-dioxolane and bicyclic-1,4-dioxane have shown potent enzyme inhibitory and antiviral activities. Inhibitor **2** ($K_i = 0.11$ nM; $IC_{50} = 3.8$ nM) displayed very potent antiviral activity in this series. While inhibitor **3** showed comparable enzyme inhibitory activity ($K_i = 0.18$ nM) its antiviral activity ($IC_{50} = 170$ nM) was significantly weaker than inhibitor **2**. Inhibitor **2** maintained an antiviral potency against a series of multi-drug resistant clinical isolates comparable to amprenavir. A protein–ligand X-ray structure of **3**-bound HIV-1 protease revealed a number of key hydrogen bonding interactions at the S2-subsite. We have created an active model of inhibitor **2** based upon this X-ray structure.

Introduction

The proteolytic enzyme HIV-1 protease is essential for viral assembly and maturation.¹ As a consequence, the design of specific inhibitors for HIV-1 protease has become the subject of immense interest. In 1996, protease inhibitors (PIs) were introduced in combination with reverse transcriptase inhibitors to become a highly active antiretroviral therapy (HAART).² This treatment regimen significantly increased life expectancy, improved quality of life and decreased mortality and morbidity among HIV/AIDS patients. Despite these notable advances, the emergence of drug-resistant HIV-1 variants is severely limiting the efficacy of HAART treatment regimens. Therefore, the development of new broad-spectrum antiretroviral drugs that produce minimal adverse effects remains an important therapeutic objective for the treatment of HIV/AIDS.³ We have recently reported our structure-based design and development of a series of novel HIV-1 protease inhibitors including darunavir,^{4,5} TMC-126,⁶ and GRL-06579A (**1**, Fig. 1).⁷ These inhibitors were designed with specific features

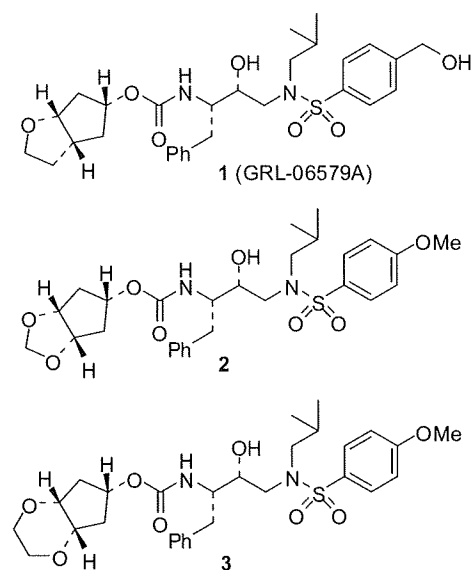


Fig. 1 Structure of inhibitors 1–3.

to help combat drug resistance. They have exhibited marked potency in enzyme inhibitory and cell-culture assays. Furthermore, these inhibitors have shown impressive activity against a broad-spectrum of HIV isolates including a variety of multi-PI-resistant clinical strains. Darunavir has been recently approved for the therapy of HIV/AIDS patients who are harboring drug-resistant HIV and do not respond to other antiretroviral drugs.

^aDepartments of Chemistry and Medicinal Chemistry, Purdue University, West Lafayette, IN 47907, USA. E-mail: akghosh@purdue.edu; Fax: +1 765 4961612; Tel: +1 765 4945323

^bDepartment of Biology, Molecular Basis of Disease, Georgia State University, Atlanta, Georgia 30303, USA

^cKumamoto University School of Medicine, Kumamoto 860-8556, Japan and Department of Hematology and Infectious Diseases

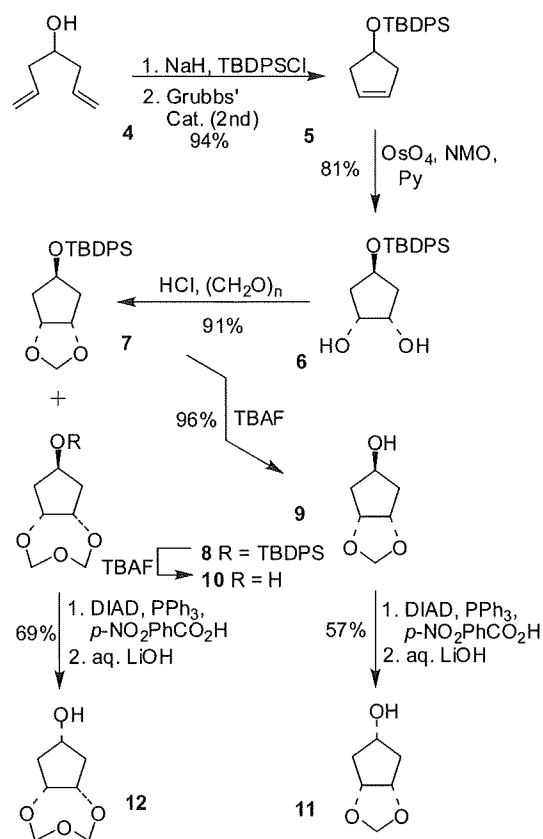
^dExperimental Retrovirology Section, HIV and AIDS Malignancy Branch, National Cancer Institute, Bethesda, Maryland 20892, USA

† Electronic supplementary information (ESI) available: HPLC and HRMS data of inhibitors 2–3 and 26–30; crystallographic data collection and refinement statistics. See DOI: 10.1039/b809178a

One of our design principles to combat drug resistance is to maximize the ligand-binding interactions in the active site and particularly to promote extensive hydrogen bonding with the active site protein backbone. Indeed, inhibitor **1** incorporates a stereochemically defined bicyclic cyclopentanyltetrahydrofuran (Cp-THF) as the P2-ligand in the hydroxyethylsulfonamide isostere. The protein–ligand X-ray structure of inhibitor **1** revealed extensive hydrogen bonding interactions with the backbone atoms throughout the enzyme active site.⁸ The cyclic ether oxygen is involved in hydrogen bonding with the backbone NH of Asp29. The presence of this oxygen is critical for its superb antiviral properties, especially against drug resistant HIV strains. Based upon further examination of the protein–ligand X-ray structure of **1**-bound HIV-1 protease, we subsequently speculated that a simplified *meso*-hexahydrocyclopenta-1,3-dioxolane ligand could conceivably maintain similar interactions with respect to the Cp-THF ligand in inhibitor **1**. Particularly, it appears that one of the oxygens of this *meso* ligand can hydrogen bond with the Asp29 NH. Since the Cp-THF ligand in inhibitor **1** contains three chiral centers, incorporation of a *meso* ligand as shown in inhibitor **2** would remarkably simplify the synthesis compared to the bicyclic Cp-THF ligand. Furthermore, we speculated that the second oxygen atom in the *meso*-P2-ligand could conceivably engage in further interactions at the S2-subsite. Herein, we report the design, synthesis and biological investigation of a series of protease inhibitors that incorporate structure-based designed symmetrical *meso*-bicyclic 1,3-dioxolane and 1,3-dioxane derivatives as the P2-ligands. Inhibitors (**2** and **3**) incorporating these ligands have shown exceedingly potent enzyme inhibitory potency as well as antiviral activity. Furthermore, we evaluated the drug-resistance profile of inhibitor **2** against multi-drug-resistant clinical isolates and it was shown to maintain tremendous potency. The protein–ligand X-ray structure of **3**-bound HIV-1 protease has been determined and this structure has provided molecular insight into the ligand-binding site interactions.

Chemistry

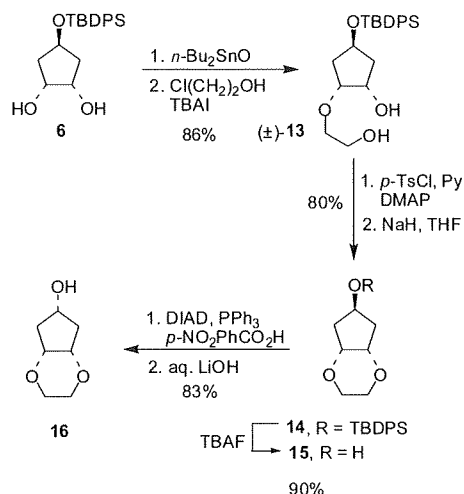
The hexahydrocyclopenta-1,3-dioxolan-5-ol (**11**), required for the synthesis of **2**, was prepared as described in Scheme 1. Commercially available 1,6-heptadien-4-ol **4** was protected as the corresponding *t*-butyldiphenylsilyl ether using sodium hydride as the base in THF. The resulting diene was subjected to a ring closing metathesis reaction using second generation Grubbs' catalyst to afford the protected cyclopenten-1-ol **5** in 94% overall yield. Osmium tetroxide-promoted dihydroxylation of olefin **5** was accomplished using a catalytic amount of osmium tetroxide and NMO and pyridine to afford diol **6** as a 6 : 1 mixture of *anti*- and *syn*-isomers which were easily separated by column chromatography. The *anti*- isomer **6** was subsequently treated with paraformaldehyde, preliminarily cracked with aqueous hydrochloric acid in chloroform under reflux,⁹ affording the cyclic acetal **7** in good yield. Along with the desired compound **7**, the trioxepane **8** was also isolated from the reaction mixture in a 1 : 1 ratio. We therefore decided to incorporate the tetrahydro-5a*H*-cyclopenta[*f*][1,3,5]trioxepan-7-yl-moiety as a P2-ligand (resulting in inhibitors **27–28**, Table 1) because the higher flexibility of the trioxepane ring could allow an improved adaptability to enzyme amino acid mutations, leading to better activity against HIV-



Scheme 1 Synthesis of alcohols 9–12.

resistant strains. Accordingly, both intermediates **7** and **8** were deprotected using tetrabutylammonium fluoride (TBAF) in THF to provide the *anti*-alcohols **9** and **10**. Compounds **9** and **10** were subsequently subjected to Mitsunobu inversion to afford the corresponding *syn*-alcohols **11** and **12**.

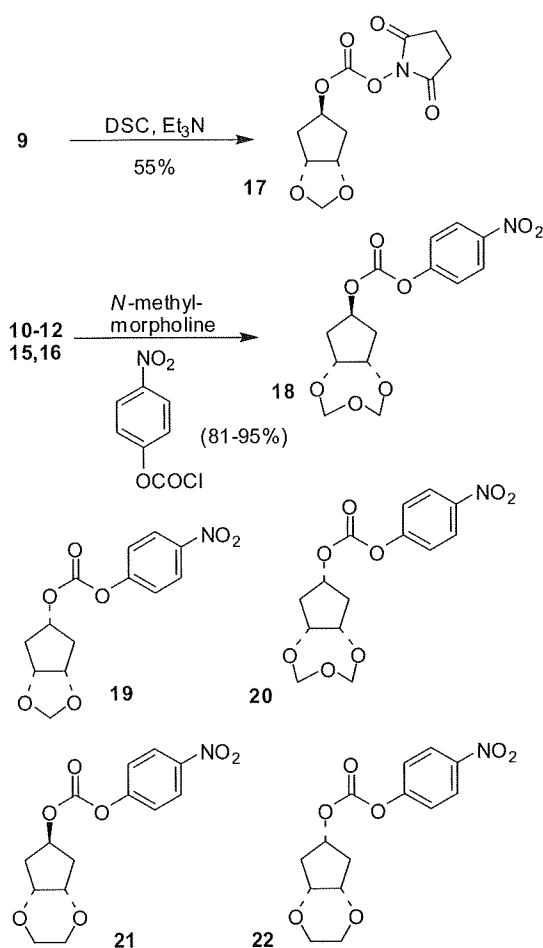
For the preparation of inhibitors **3** and **29**, alcohols **15** and **16** were synthesized as described in Scheme 2. Diol **6** was heated under reflux in toluene in the presence of dibutyltin oxide with azeotropic removal of water. The resulting stannylene acetal intermediate was treated with chloroethanol to obtain the monoalkylated derivative **13** in 68% overall yield.¹⁰ Subsequently, the primary



Scheme 2 Synthesis of alcohols **15** and **16**.

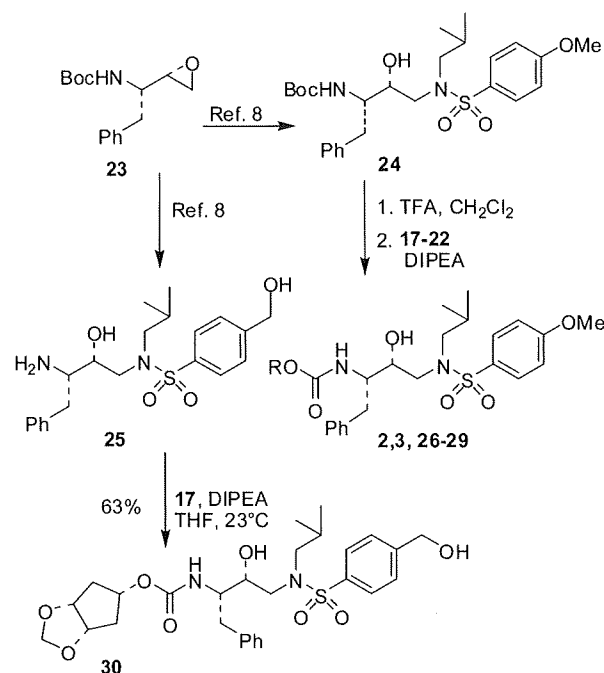
alcohol was selectively tosylated with *p*-toluenesulfonyl chloride in the presence of pyridine. Exposure of the resulting compound to sodium hydride resulted in an intramolecular substitution reaction leading to the corresponding cyclization compound **14**. TBAF-mediated deprotection furnished the target *anti*-alcohol **15** in good overall yield. The *syn*-alcohol **16** was then obtained after Mitsunobu inversion of **15** as described above.

The synthesis of the active carbonates required for the synthesis of the various inhibitors is shown in Scheme 3. Alcohol **9** was converted to the succinimidyl-derivative **17** by treatment with *N,N'*-succinimidylcarbonate in the presence of Et₃N as described previously.¹¹ Alcohols **10–12**, **15** and **16** were activated by conversion to the corresponding *p*-nitrophenylcarbamates **18–22** (81–95% yield) by using *p*-nitrophenylchloroformate and *N*-methylmorpholine in THF. The general procedure for the synthesis of inhibitors **2**, **3** and **26–30** is outlined in Scheme 4. Epoxide **23**¹² was converted into intermediate **24** following our previously reported procedure.⁸ Deprotection of **24** by using trifluoroacetic acid followed by reaction with the activated alcohols **17–22** furnished inhibitors **2**, **3** and **26–29** in 43–85% yields.



Scheme 3 Synthesis of activated alcohols **17–22**.

Finally, inhibitor **30** was synthesized from the known⁸ amine **25**. This amine was reacted with the activated carbonate **17** in the presence of diisopropylethylamine in THF at 23 °C to provide **30**. Inhibitor **30** was obtained in 63% yield.



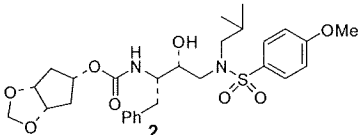
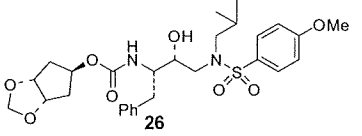
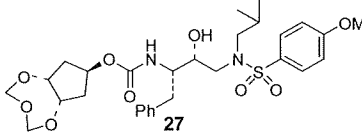
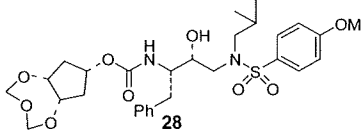
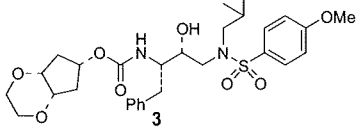
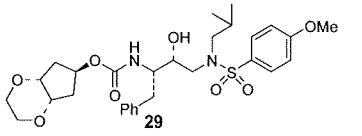
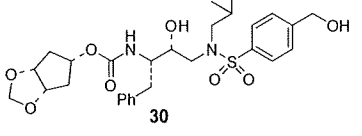
Scheme 4 Synthesis of inhibitors **2**, **3** and **26–30**.

Results and discussion

The inhibitory potencies of the synthetic inhibitors were evaluated using the assay protocol of Toth and Marshall,¹³ and the results are shown in Table 1. As can be seen, inhibitor **2** has shown an enzyme inhibitory potency of 0.11 nM. It appears that the bicyclic 1,3-dioxolane ring can be accommodated by the S2-subsite of HIV-1 protease. Inhibitor **26** with a *meso* ligand containing a *trans*-bicyclic-1,3-dioxolane ring is 2.5-fold less potent than the *syn*-isomer **2**. We have examined the effect of both *syn* and *anti*-trioxepane rings as P2-ligands in inhibitors **27** and **28**. The *syn*-isomer **28** is significantly more potent ($K_i = 0.51$ nM) than the *anti*-isomer **27**. Considering the acid sensitivity of 1,3-dioxolane rings, we not only speculated that the stable 1,4-dioxane ring may fill the hydrophobic S2-site, but also that the oxygens on the dioxane ring may interact with backbone atoms or residues in the active site. As shown, the *meso* ligand in inhibitor **3** with a *syn*-bicyclic-1,4-dioxane ring has shown an enzyme inhibitory potency of 0.18 nM (K_i value). Consistent with previous results, the corresponding *anti*-isomer **29** is significantly less potent. As reported previously, the P2-ligand Cp-THF with a P2'-hydroxymethyl sulfonamide (inhibitor **1**) is significantly more potent than the corresponding P2'-methoxybenzene sulfonamide derivative. We have, therefore, compared the inhibitory potency of inhibitor **30**, containing a P2'-hydroxymethyl benzene sulfonamide derivative, with inhibitor **2**. However, inhibitor **30** did not exhibit this potency enhancing effect.

We have examined selected compounds for their activity against HIV-1 using a human CD4+ T-cell line (MT-2 cells). The activity of inhibitor **2** against a variety of multi-drug-resistant HIV-1 variants was also examined in detail using human peripheral blood mononuclear cells (PBMCs) as target cells. We employed two endpoints for the activity against HIV-1: (i) the inhibition of the HIV-1-elicited cytopathic effect for MT-2 cells and (ii) the inhibition of HIV-1 p24 production for PBMCs.⁵

Table 1 Enzymatic inhibitory activity of compounds **2**, **3**, **26–30** and antiviral activity of selected inhibitors against HIV-1_{LAI}

Entry	Inhibitor	K_i /nM ^a	IC ₅₀ /μM ^b
1		0.11 ± 0.01	0.0038 ± 0.0001
2		0.40 ± 0.04	nd
3		5.4 ± 0.22	>1
4		0.51 ± 0.01	0.38 ± 0.02
5		0.18 ± 0.03	0.21 ± 0.04
6		0.50 ± 0.04	nd
7		0.34 ± 0.07	0.0077 ± 0.003

^a Values are means of at least two experiments. ^b MT-2 human T-lymphoid cells exposed to HIV-1_{LAI}; antiviral activity of amprenavir (APV), saquinavir (SQV) and indinavir (IDV) were 0.03 μM, 0.02 μM and 0.03 μM respectively in this assay. nd: not determined.

When examined in MT-2 cells as the target cells, inhibitor **2** displayed an impressive antiviral IC₅₀ of 3.8 nM (Table 1). Inhibitor **3** showed an antiviral IC₅₀ value in the high nanomolar range (IC₅₀ = 210 nM, Table 1), while it exhibited a similar K_i to inhibitor **2**. We subsequently examined inhibitor **2** for its activity against a clinical wild-type X4-HIV-1 isolate (HIV-1_{ERS104pre}) along with various multi-drug-resistant clinical X4- and R5-HIV-1 isolates (Table 2) using PBMCs as the target cells.⁵ The activity of inhibitor **2** against HIV-1_{ERS104pre} (IC₅₀ = 29 nM) was comparable to those of currently available protease inhibitors, SQV, APV, and IDV, which display IC₅₀ values of 12, 33, and 26 nM, respectively. Of particular note, the IC₅₀ value of inhibitor **2** in PBMCs (IC₅₀ = 29 nM) was nearly 8-fold greater than the IC₅₀ value in MT-2 cells

(IC₅₀ = 3.8 nM). With regard to this difference, considering that **2** is highly potent as examined in human T-cells (MT-2 cells) but its activity is slightly less in PBMCs, it is possible that relatively higher concentrations of **2** are required to suppress HIV-1 production in chronically infected macrophages.¹⁴ IDV was not capable of efficiently suppressing the replication of most of the multi-drug-resistant clinical isolates examined (HIV-1_{MDR/MM}, HIV-1_{MDR/ISL}, HIV-1_{MDR/C}, and HIV-1_{MDR/A}), with IC₅₀ values of >1.0 μM. The potency of inhibitor **2** against most of the multi-drug-resistant variants was generally comparable to that of SQV and APV, although DRV was found to be the most potent among those tested, including inhibitor **2**, against HIV-1_{ERS104pre} as well as all the multi-drug-resistant variants.

Table 2 Antiviral activity of inhibitor **2** against clinical HIV-1 isolates in PBMC cells

Virus ^b	IC ₅₀ values ^a (nM)				
	2	DRV ^c	SQV ^d	APV ^e	IDV ^f
HIV-1 _{ERS104pre} (wild-type; X4)	29	3,5	12	33	26
HIV-1 _{MDR/MM} (R5)	150 (5)	17 (5)	190 (16)	300 (9)	>1000 (>38)
HIV-1 _{MDR/JSL} (R5)	550 (19)	26 (7)	330 (28)	430 (13)	>1000 (>38)
HIV-1 _{MDR/C} (X4)	300 (10)	7 (2)	36 (3)	230 (7)	>1000 (>38)
HIV-1 _{MDR/G} (X4)	340 (12)	7 (2)	29 (2)	340 (10)	290 (11)
HIV-1 _{MDR/A} (X4)	21 (1)	3 (1)	81 (7)	100 (3)	>1000 (>38)

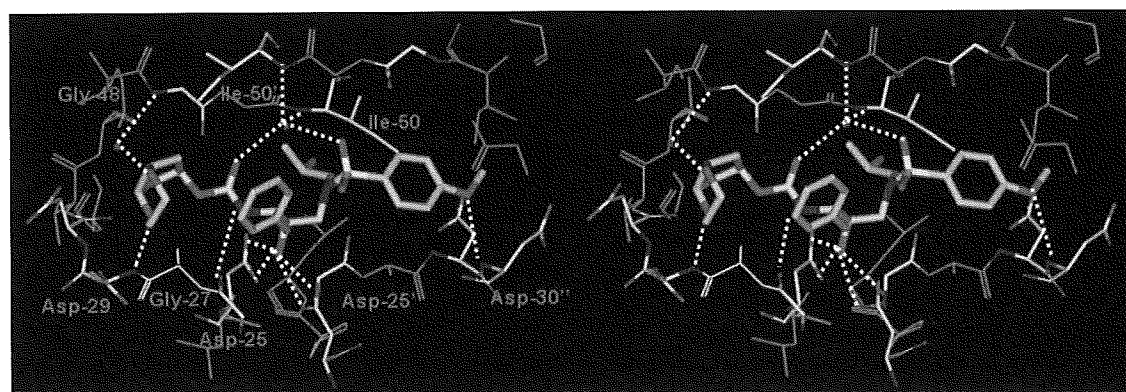
^a Amino acid substitutions identified in the protease-encoding region compared to the consensus type B sequence cited from the Los Alamos database include L63P in HIV-1_{ERS104pre}; L10I, K43T, M46L, I54V, L63P, A71V, V82A, L90M, and Q92K in HIV-1_{MDR/MM}; L10I, L24I, I33F, E35D, M36I, N37S, M46L, I54V, R57K, I62V, L63P, A71V, G73S, and V82A in HIV-1_{MDR/JSL}; L10I, I15V, K20R, L24I, M36I, M46L, I54V, I62V, L63P, K70Q, V82A, and L89M in HIV-1_{MDR/C}; L10I, V11I, T12E, I15V, L19I, R41K, M46L, L63P, A71T, V82A, and L90M in HIV-1_{MDR/G}; and L10I, I15V, E35D, N37E, K45R, I54V, L63P, A71V, V82T, L90M, I93L, and C95F in HIV-1_{MDR/A}. HIV-1_{ERS104pre} served as a source of wild-type HIV-1. The IC₅₀ values were determined by employing PHA-PBMC (phytohemagglutinin-activated peripheral blood mononuclear cells) as target cells and the inhibition of p24Gag protein production as the endpoint. All values were determined in triplicate. ^b X4 denotes CXCR4-tropic HIV-1 while R5 CCR5-tropic HIV-1. ^c DRV (darunavir). ^d SQV (saquinavir). ^e APV (amprenavir). ^f IDV (indinavir).

X-Ray crystallography

To obtain molecular insight into the ligand-binding site interactions responsible for the impressive enzyme inhibitory potency of compound **3**, we determined the X-ray structure of **3**-bound HIV-1 protease. The crystal structure was solved and refined to an *R* factor of 15.2% at a 1.07 Å resolution. The inhibitor binds with extensive interactions from P2 to P2' with the protease atoms, and most notable are the favorable polar interactions including hydrogen bonds, as shown in Fig. 2. The transition-state hydroxyl group forms hydrogen bonds to the side chain carboxylate oxygen atoms of the catalytic Asp25 and Asp25'. Of particular interest, the *meso*-bicyclic 1,4-dioxane ligand appears to be involved in hydrogen bonding interactions with the backbone atoms and residues at the S2-site. One of the dioxane oxygens hydrogen bonds with the backbone NH of Asp29. The other oxygen makes a water-mediated hydrogen bond with the carbonyl oxygen of Gly48. These interactions are described in several peptide substrate analogs.¹⁵ However, the design of high affinity ligands incorporating this interaction with Gly48 has not been previously demonstrated. The inhibitor also hydrogen bonds with the protease main chain amide carbonyl oxygen of Gly27, and there are water-mediated interactions with the amides of Ile50 and Ile50' that are conserved in the majority of protease complexes with inhibitors¹⁶ and

substrate analogs.¹⁵ The weaker polar interactions such as C–H...O and water- π interactions can be analyzed accurately in atomic resolution structures.^{17,18} Inhibitor **3** also shows a water-mediated interaction of the π system of the P2' aromatic ring with the amide of Asp29', which was also observed for darunavir and inhibitor **1**.¹⁹ Furthermore, the P2' methoxy group forms a hydrogen bond to the backbone NH of Asp30'. Importantly, the P2 group forms a hydrogen bond interaction with the carbonyl oxygen of Gly48 and a water-mediated interaction with the amide of Gly48, similar to the interactions described for several peptide substrate analogs.¹⁵ These interactions of the P2 group confirm the design strategy of incorporating new polar interactions with conserved backbone regions of the protease.

In an effort to understand the binding interactions of the corresponding *meso*-1,3-dioxolane ligand in the S2-subsite, we have created an active model of inhibitor **2** (Fig. 3) based upon the X-ray structure of **3**-bound HIV-1 protease. The model suggests that both dioxolane oxygens may interact with both active site residues Asp29 and Asp30, as well as Gly48 through the structural water molecule. In comparison, it appears that the dioxane oxygens of inhibitor **3** are not within hydrogen bonding distance of the backbone NH of Asp30. This may explain the marked difference in antiviral activity of inhibitor **2** compared with inhibitor **3**.

**Fig. 2** Stereoview of the X-ray structure of inhibitor **3** bound to the active site of wild-type HIV-1 protease.

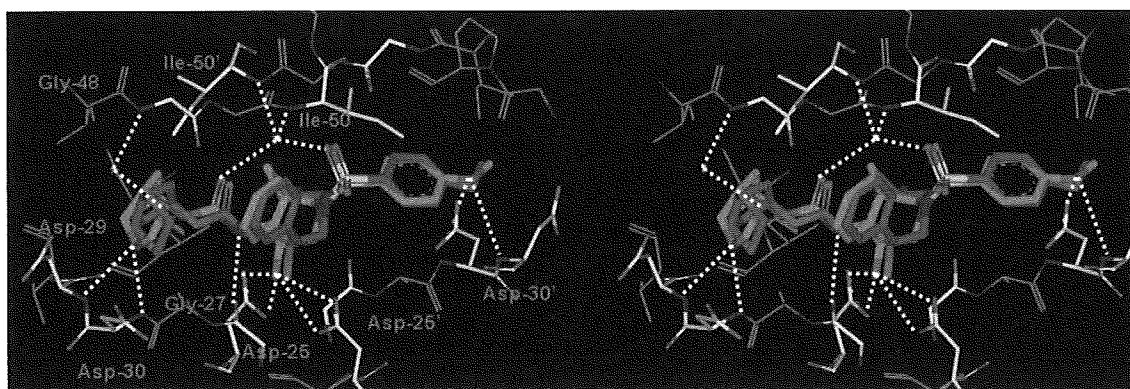


Fig. 3 A stereoview of an active model of inhibitor 2 (green) with the X-ray structure of inhibitor 3 (magenta)-bound HIV-1 protease.

Conclusions

In summary, a series of novel HIV-1 protease inhibitors were designed and synthesized by incorporating bicyclic *meso*-1,3-dioxolane and 1,4-dioxane derivatives as the P2-ligands. A number of inhibitors have shown very impressive enzyme inhibitory and antiviral potency, similar to inhibitor 1 with a stereochemically defined Cp-THF ligand. The design of *meso*-1,3-dioxolane and 1,4-dioxane P2-ligands as exemplified in inhibitors 2 and 3, respectively, has remarkably simplified the stereochemical complexity as well as chemical synthesis over the Cp-THF ligand in inhibitor 1. We have developed efficient synthetic routes to these ligands. Inhibitor 2 has shown potent antiviral activity in both MT-2 cells and PBMCs. Inhibitor 2 was profiled against a series of multi-drug-resistant clinical isolates. While inhibitor 2 is less potent than darunavir, it is significantly more potent than IDV and comparable to APV and SQV in suppressing the replication of multi-drug-resistant isolates MDR_{MM} and MDR_{JSL}. A protein–ligand X-ray structure of 3-bound HIV-1 protease revealed extensive interactions of the inhibitor with the active site of HIV-1 protease. Most notably, both oxygens of the *meso*-P2-ligand are involved in hydrogen bonding interactions with the protein backbone atoms. In particular, a water-mediated hydrogen bond to the Gly48 carbonyl is very unique. An active model of inhibitor 2 indicates similar ligand binding site interactions. Our design principle of increasing ‘backbone binding’ appears to maintain key interactions in the enzyme active site leading to retained potency against multi-drug-resistant variants. Further design and ligand optimization involving these interactions is in progress.

Experimental

General. All moisture sensitive reactions were carried out under a nitrogen or argon atmosphere. Anhydrous solvents were obtained as follows: THF, diethyl ether, and benzene, distilled from sodium and benzophenone; dichloromethane, pyridine, triethylamine, and diisopropylethylamine, distilled from CaH₂. All other solvents were HPLC grade. Column chromatography was performed with Whatman 240–400 mesh silica gel under low pressure (5–10 psi). TLC was carried out with E. Merck silica gel 60 F₂₅₄ plates. ¹H and ¹³C NMR spectra were recorded on Varian Mercury 300 and Bruker Avance 400 and 500 spectrom-

eters. Optical rotations were measured using a Perkin-Elmer 341 polarimeter. IR spectra were recorded on a Matteson Genesis II FT-IR spectrometer.

4-(*tert*-Butyldiphenylsilyloxy)-4*H*-cyclopentene (5)

To a suspension of sodium hydride (60% in mineral oil, 0.92 g, 23 mmol) in THF (10 mL), cooled to 0 °C, 1,6-heptadien-4-ol 4 (1 mL, 7.7 mmol) was added dropwise over 10 min. The resulting suspension was stirred at 0 °C for 30 min and then *tert*-butyldiphenylchlorosilane (2 mL, 7.9 mmol) was added. The reaction mixture was stirred at 23 °C for 4 h and then quenched with a saturated solution of ammonium chloride. The solvent was removed *in vacuo* and the aqueous phase was extracted with CH₂Cl₂. The organic extracts were dried (Na₂SO₄), the solvent removed and the residue purified by flash-chromatography (1 : 10, EtOAc–Hex) to afford 4-(*tert*-butyldiphenylsilyloxy)hepta-1,6-diene (2.6 g, 96%) as a colorless oil: IR ν_{\max} (NaCl; cm⁻¹) 3066, 2951, 1421, 1103 and 696; δ_{H} (300 MHz, CDCl₃) 7.70 (4 H, dd, *J* 1.6, 7.6 Hz, ArH), 7.47–7.38 (6 H, m, ArH), 5.83–5.69 (2 H, m, 2 × CH=CH₂), 5.02–4.91 (4 H, m, 2 × CH=CH₂), 3.87–3.80 (1 H, m, CHOSi), 2.31–2.12 (4 H, m, 3-H₂, 5-H₂) and 1.08 [9 H, s, C(CH₃)₃]; δ_{C} (75 MHz, CDCl₃) 135.9, 134.7, 134.3, 129.5, 127.5, 117.1, 72.4, 40.5, 27.0 and 19.4; *m/z* (CI) 351 (M + H, 100); HRMS (M + H)⁺ calcd for C₂₃H₃₁OSi, 351.2144; found, 351.2146.

To a solution of the above compound (2.0 g, 5.7 mmol) in dry CH₂Cl₂ (20 mL), second generation Grubbs' catalyst (48 mg) was added and the resulting mixture was heated under reflux for 2 h. Subsequently, the reaction mixture was cooled to 23 °C, the solvent removed under reduced pressure and the residue purified by flash-chromatography (1 : 10 EtOAc–Hex) to afford 5 (1.8 g, 98%) as a colorless oil: IR ν_{\max} (NaCl; cm⁻¹) 3067, 2853, 2736, 1428, 1109 and 702; δ_{H} (300 MHz, CDCl₃) 7.67 (4 H, dd, *J* 1.8, 7.8, ArH), 7.45–7.34 (6 H, m, ArH), 5.61 (2 H, s, 1-H, 2-H), 4.57–4.51 (1 H, m, 4-H), 2.47–2.33 (4 H, m, 3-H₂, 5-H₂) and 1.05 [9 H, s, C(CH₃)₃]; δ_{C} (100 MHz, CDCl₃) 135.7, 134.5, 129.5, 128.3, 127.5, 73.5, 42.4, 26.9 and 19.1; *m/z* (CI) 323 (M + H, 100); HRMS (M + H)⁺ calcd for C₂₁H₂₇OSi, 323.1831; found, 323.1834.

(1*α*,2*α*,4*β*)-4-(*tert*-Butyldiphenylsilyloxy)-1,2-cyclopentanediol (6)

A mixture of 5 (5.1 g, 15.8 mmol), osmium tetroxide (2.5 wt% solution in *tert*-butanol, 4 mL), *N*-methylmorpholine-*N*-oxide (2.6 g, 22.2 mmol), and pyridine (1.3 mL, 15.8 mmol) in a

3 : 2 : 1 mixture of *tert*-butanol, THF, and water (80 mL) was heated under reflux for 4 h. The reaction mixture was cooled to 23 °C and treated with a 20% aqueous solution of sodium bisulfite (10 mL). The organic solvents were removed under reduced pressure and the aqueous phase was extracted with EtOAc. The organic extracts were washed with 1 N hydrochloric acid, water and brine, and dried (Na₂SO₄). The solvent was removed *in vacuo* and the residue was purified by flash-chromatography (1 : 1 EtOAc–Hex) to yield diol **6** (5.3 g, 94%) as a colorless oil: IR ν_{\max} (NaCl; cm⁻¹) 3006, 2676, 1427, 1112 and 702; δ_{H} (300 MHz, CDCl₃) 7.62 (4 H, dd, *J* 1.8, 7.5, ArH), 7.45–7.33 (6 H, m, ArH), 4.84–4.42 (1 H, m, 4-H), 4.30–4.29 (2 H, m, 1-H, 2-H), 2.22 (2 H, br. s, 2 × OH), 1.99–1.80 (4 H, m, 3-H₂, 5-H₂) and 1.04 [9 H, s, C(CH₃)₃]; δ_{C} (100 MHz, CDCl₃) 135.6, 134.0, 129.6, 127.6, 72.4, 71.2, 41.9, 26.8 and 19.0; *m/z* (EI) 356 (M, 100); HRMS (M)⁺ calcd for C₂₁H₂₈O₃Si, 356.1808; found, 356.1803.

(1 β ,2 β ,4 α)-4-(*tert*-Butyldiphenylsilyloxy)-1,2-(methylenedioxy)cyclopentane (7) and (5 α ,7 β ,8 α)-7-(*tert*-butyldiphenylsilyloxy)-tetrahydrocyclopental[*f*]-1,3,5-trioxepane (8)

A mixture of paraformaldehyde (0.77 g, 25.7 mmol) and concentrated hydrochloric acid (2 mL) in CHCl₃ (2 mL) was stirred at 23 °C until a clear solution was formed (6 h) and then a solution of **6** (0.2 g, 0.54 mmol) in CHCl₃ (2 mL) was added. The resulting mixture was heated under reflux overnight and the aqueous phase was extracted with CHCl₃. The organic extracts were dried (Na₂SO₄) and evaporated under reduced pressure to yield **7** (0.18 g, 86%) after flash-chromatography (1 : 10, EtOAc–Hex): IR ν_{\max} (NaCl; cm⁻¹) 2791, 1589, 1471, 1428, 822 and 699; δ_{H} (300 MHz, CDCl₃) 7.64 (4 H, d, *J* 6.3, ArH), 7.45–7.35 (6 H, m, ArH), 4.78 (1 H, s), 4.60 (1 H, s), 4.51 (2 H, d, *J* 5.4, 1-H, 2-H), 4.47–4.39 (1 H, m, 4-H), 1.99 (2 H, dd, *J* 6.0, 13.8, 3-H', 5-H'), 1.77–1.68 (2 H, m, 3-H'', 5-H'') and 1.04 [9 H, s, C(CH₃)₃]; δ_{C} (75 MHz, CDCl₃) 135.6, 134.0, 129.7, 127.6, 94.0, 78.8, 72.7, 41.0, 26.9 and 19.1; *m/z* (EI) 368 (M, 100). After further elution of the column **8** (0.5 g, 5%) was obtained: IR ν_{\max} (NaCl; cm⁻¹) 2827, 2726, 1427, 1113 and 703; δ_{H} (300 MHz, CDCl₃) 7.66–7.62 (4 H, m, ArH), 7.46–7.35 (6 H, m, ArH), 5.17 (2 H, d, *J* 7.8, 2-H', 4-H'), 4.70 (2 H, d, *J* 7.8, 2-H'', 4-H''), 4.52–4.43 (3 H, m, 5a-H, 7-H, 8a-H), 2.15–2.08 (2 H, m, 6-H', 8-H'), 1.93–1.85 (2 H, m, 6-H'', 8-H'') and 1.06 [9 H, s, C(CH₃)₃]; δ_{C} (75 MHz, CDCl₃) 135.6, 133.8, 129.7, 127.7, 96.1, 82.5, 71.7, 41.1, 26.9 and 19.1; *m/z* (CI) 397 (M – H, 100); HRMS (M – H)⁺ calcd for C₂₃H₂₉O₄Si, 397.1832; found, 397.1832.

(4 α ,1 β ,2 β)-4-Hydroxy-1,2-(methylenedioxy)cyclopentane (9)

A mixture of **7** (0.47 g, 1.3 mmol) and *n*-Bu₄N⁺F⁻ (1.0 M solution in THF, 1.4 mL, 1.4 mmol) in dry THF (10 mL) was stirred at 23 °C for 16 h. To the reaction mixture was added a saturated solution of NaHCO₃, the solvent was removed *in vacuo* and the aqueous phase extracted with Et₂O. The organic extracts were dried (Na₂SO₄) and evaporated and the residue was purified by flash-chromatography (1 : 1 EtOAc–Hex) to yield **9** (0.16 g, 96%) as a colorless oil: IR ν_{\max} (NaCl; cm⁻¹) 3044, 2792, 2602, 1065, 821 and 602; δ_{H} (300 MHz, CDCl₃) 4.89 (1 H, s, OCHHO), 4.59 (1 H, s, OCHHO), 4.50 (2 H, d, *J* 6.0, 1-H, 2-H), 4.41–4.32 (1 H, m, 4-H), 3.13 (1 H, br. s, OH), 2.09 (2 H, dd, *J* 5.6, 14.0, 3-H', 5-H')

and 1.61–1.51 (2 H, m, 3-H'', 5-H''); δ_{C} (75 MHz, CDCl₃) 94.1, 78.9, 70.8 and 40.6; *m/z* (CI) 129 (M – H, 100); HRMS (M – H)⁺ calcd for C₆H₉O₃, 129.0552; found, 129.0556.

(5 α ,7 β ,8 α)-7-Hydroxytetrahydrocyclopental[*f*]-1,3,5-trioxepane (10)

The title compound was obtained as described for **9** in 83% yield. Flash-chromatography was performed using EtOAc: IR ν_{\max} (NaCl; cm⁻¹) 3036, 2649, 1424, 1118 and 930; δ_{H} (300 MHz, CDCl₃) 5.15 (2 H, d, *J* 7.2, 2-H', 4-H'), 4.67 (2 H, d, *J* 7.2, 2-H'', 4-H''), 4.47–4.40 (3 H, m, 5a-H, 7-H, 8a-H), 2.07–2.02 (4 H, m, 6-H₂, 8-H₂) and 1.86 (1 H, br. s, OH); δ_{C} (75 MHz, CDCl₃) 96.1, 82.3, 70.0 and 40.8; *m/z* (EI) 160 (M, 100); HRMS (M)⁺ calcd for C₇H₁₂O₄, 160.0736; found, 160.0738.

(1 β ,2 β ,4 β)-4-Hydroxy-1,2-(methylenedioxy)cyclopentane (11)

To a mixture of **9** (100 mg, 0.77 mmol), *p*-nitrobenzoic acid (250 mg, 1.5 mmol), and triphenylphosphine (450 mg, 1.5 mmol), was added diisopropylazodicarboxylate (300 μ L, 1.5 mmol) dropwise and the resulting mixture was stirred at 23 °C. After 16 h, the solvent was removed under reduced pressure and the residue purified by flash-chromatography (1 : 2 EtOAc–Hex). The resulting ester was dissolved in a 3 : 2 : 1 mixture of THF, methanol, and water (10 mL) and LiOH·H₂O (162 mg, 3.8 mmol) was added. The yellow mixture was stirred at 23 °C for 5 h and then the solvent was removed *in vacuo*. The residue was diluted with water and the aqueous phase extracted with Et₂O. The organic extracts were dried (Na₂SO₄) and the solvent was evaporated. Purification of the residue by flash-chromatography (1 : 1 EtOAc–Hex) afforded **11** (57 mg, 57%) as a colorless oil: IR ν_{\max} (NaCl; cm⁻¹) 3052, 2804, 2577, 1164, 1096, 1011 and 924; δ_{H} (300 MHz, CDCl₃) 5.17 (1 H, s, OCHHO), 4.68 (1 H, s, OCHHO), 4.61 (2 H, d, *J* 4.8, 1-H, 2-H), 4.27 (1 H, t, *J* 4.7, 4-H), 2.33 (1 H, br. s, OH), 2.21 (2 H, d, *J* 15.3, 3-H', 5-H') and 1.85–1.77 (2 H, m, 3-H'', 5-H''); δ_{C} (75 MHz, CDCl₃) 94.7, 81.5, 74.0 and 41.0; *m/z* (EI) 129 (M – H, 100); HRMS (M – H)⁺ calcd for C₆H₉O₃, 129.0611; found, 129.1012.

(5 α ,7 α ,8 α)-7-Hydroxytetrahydrocyclopental[*f*]-1,3,5-trioxepane (12)

The title compound **12** was obtained as described for **11** in 69% yield. Flash-chromatography was performed using EtOAc: IR ν_{\max} (NaCl; cm⁻¹) 3044, 2832, 2633, 1481, 1116 and 928; δ_{H} (300 MHz, CDCl₃) 5.18 (2 H, d, *J* 7.2, 2-H', 4-H'), 4.67 (2 H, d, *J* 7.2, 2-H'', 4-H''), 4.31–4.25 (2 H, m, 5a-H, 8a-H), 4.18–4.13 (1 H, m, 7-H), 2.40 (1 H, br. s, OH), 2.17–2.08 (2 H, m, 6-H', 8-H') and 2.03–1.96 (2 H, m, 6-H'', 8-H''); δ_{C} (75 MHz, CDCl₃) 95.3, 82.8, 71.0 and 41.1; *m/z* (CI) 161 (M + H, 100); HRMS (M + H)⁺ calcd for C₇H₁₂O₄, 161.0814; found, 161.0814.

(\pm)-(1 β ,2 β ,4 α)-2-(2'-Hydroxyethoxy)-4-(*tert*-butyldiphenylsilyloxy)cyclopentane-1-ol (13)

A mixture of **6** (1.4 g, 3.9 mmol) and dibutyltin oxide (0.94 g, 3.9 mmol) in dry toluene (130 mL) was heated under reflux with azeotropic removal of water. After 5 h, the reaction mixture was concentrated to half the initial volume and chloroethanol (2.5 mL,

39 mmol) and *n*-Bu₄N⁺I⁻ (1.4 g, 3.9 mmol) were added. The resulting mixture was heated under reflux for 19 h. Afterwards the solvent was evaporated and the residue was purified by flash-chromatography (10 : 1 EtOAc–MeOH) to afford **13** (1.3 g, 86%) as a colorless oil: IR ν_{\max} (NaCl; cm⁻¹) 3102, 2604, 1589, 1471, 1062, 823 and 612; δ_{H} (300 MHz, CDCl₃) 7.62 (4 H, d, *J* 8.7, ArH), 7.44–7.33 (6 H, m, ArH), 4.45–4.40 (1 H, m, 4-H), 4.33–4.28 (1 H, m, 2-H), 4.04–3.98 (1 H, m, 1-H), 3.76–3.71 (2 H, m, CH₂O), 3.66–3.55 (2H, m, CH₂O), 3.01 (2 H, br. s, 2 × OH), 1.97–1.80 (4 H, m, 3-H₂, 5-H₂) and 1.04 (s, 9H); δ_{C} (75 MHz, CDCl₃) 135.6, 134.1, 129.6, 127.6, 80.7, 71.1, 71.0, 70.8, 61.7, 42.3, 39.0, 26.9 and 14.2; *m/z* (ESI) 423 (M + Na, 100).

(1β,2β,4α)-4-(*tert*-butyldiphenylsilyloxy)-1,2-(ethylenedioxy)-cyclopentane (14)

A mixture of **13** (1.2 g, 3.0 mmol), *p*-toluenesulfonyl chloride (1.3 mg, 6.6 mmol), pyridine (1.2 mL, 15 mmol) and a catalytic amount of *N,N*-dimethylaminopyridine in CH₂Cl₂ (40 mL) was stirred at 23 °C for 24 h. The reaction mixture was treated with 1 N HCl and the aqueous phase was extracted with CH₂Cl₂. The organic extracts were dried (Na₂SO₄) and the solvent removed. Purification of the residue by flash-chromatography (1 : 1 EtOAc–Hex) afforded the tosylated alcohol (990 mg, 60%) as a colorless oil: IR ν_{\max} (NaCl; cm⁻¹) 3104, 2992, 2691, 1598, 1359, 1177, 923 and 705; δ_{H} (300 MHz, CDCl₃) 7.76 (2 H, d, *J* 8.4, ArH), 7.61 (4 H, d, *J* 7.8, ArH), 7.42–7.26 (8 H, m, ArH), 4.53–4.25 (1 H, m, CHO), 4.15–4.09 (3 H, m, CHO, CH₂O), 3.96–3.91 (1 H, m, CHO), 3.68–3.62 (2 H, m, CH₂O), 2.41 (3 H, s, CH₃), 1.89–1.75 (4 H, m, 3-H₂, 5-H₂) and 1.03 [9 H, s, C(CH₃)₃]; δ_{C} (100 MHz, CDCl₃) 135.6, 134.0, 132.8, 129.8, 129.6, 127.9, 127.8, 127.6, 80.7, 71.3, 71.0, 69.0, 68.6, 67.0, 42.1, 38.7, 26.8, 21.6 and 18.9. To a solution of the above product (150 mg, 0.27 mmol) in dry THF (12 mL), NaH (60% in mineral oil, 22 mg, 0.54 mmol) was added and the resulting suspension was heated under reflux for 30 min. After cooling to 23 °C, the reaction mixture was quenched with a saturated solution of NH₄Cl, the solvent was removed and the aqueous phase was extracted with EtOAc. The organic extracts were dried (Na₂SO₄) and the solvent was removed *in vacuo*. The residue was purified by flash-chromatography (1 : 3 EtOAc–Hex) to afford **14** (82 mg, 80%) as a colorless oil: IR ν_{\max} (NaCl; cm⁻¹) 2803, 1427, 1136, 957 and 703; δ_{H} (300 MHz, CDCl₃) 7.65 (4 H, d, *J* 7.8, ArH), 7.46–7.36 (6 H, m, ArH), 4.55–4.48 (1 H, m, 4-H), 4.18 (2 H, t, *J* 5.1, 1-H, 2-H), 3.70–3.62 (2 H, m, CH₂O), 3.53–3.46 (2 H, m, CH₂O), 2.16–2.07 (2 H, m, 3-H', 5-H'), 1.82–1.74 (2 H, m, 3-H'', 5-H'') and 1.06 [9 H, s, C(CH₃)₃]; δ_{C} (75 MHz, CDCl₃) 135.6, 134.1, 129.5, 127.6, 75.2, 71.1, 62.2, 37.5, 27.0 and 19.1; *m/z* (CI): 383.25 (M + H, 100).

(1β,2β,4α)-4-Hydroxy-1,2-(ethylenedioxy)cyclopentane (15)

The above compound was deprotected as described for **9** to afford **15** in 90% yield as a colorless oil: IR ν_{\max} (NaCl; cm⁻¹) 3013, 2797, 2550, 1129 and 664; δ_{H} (300 MHz, CDCl₃) 4.58–4.51 (1 H, m, 4-H), 4.17 (2 H, t, *J* 4.8, 1-H, 2-H), 3.78–3.71 (2 H, m, CH₂O), 3.58–3.51 (2 H, m, CH₂O), 2.34–2.25 (2 H, m, 3-H', 5-H') and 1.72–1.66 (3 H, m, 3-H'', 5-H'', OH); δ_{C} (75 MHz, CDCl₃) 75.1, 69.6, 62.3 and 37.2; *m/z* (EI) 144 (M, 100).

(1β,2β,4β)-4-Hydroxy-1,2-(ethylenedioxy)cyclopentane (16)

Starting from **15** the title compound **16** was obtained as described for **11** in 83% yield as a colorless oil. Flash-chromatography was performed using EtOAc: IR ν_{\max} (NaCl; cm⁻¹) 3014, 2571, 1135, 1081 and 875; δ_{H} (300 MHz, CDCl₃) 4.22–4.16 (1 H, m, 4-H), 4.01 (2 H, t, *J* 4.2, 1-H, 2-H), 3.88–3.80 (2 H, m, CH₂O), 3.63–3.55 (2 H, m, CH₂O), 2.57 (1 H, br. s, OH) and 2.10–1.93 (4 H, m, 3-H₂, 5-H₂); δ_{C} (75 MHz, CDCl₃) 76.0, 71.4, 62.3 and 37.5; *m/z* (EI) 144 (M, 100).

(1β,2β,4β)-1,2-(Methylenedioxy)cyclopent-4-yl succinimidylcarbonate (17)

To a solution of **9** (67 mg, 0.52 mmol) in dry acetonitrile (2 mL), *N,N'*-disuccinimidyl carbonate (198 mg, 0.77 mmol) and triethylamine (145 μL, 1.0 mmol) were added and the resulting mixture was stirred at 23 °C. After 8 h the solvent was removed, the residue was taken up in a saturated solution of NaHCO₃ and the aqueous phase was extracted with EtOAc. The organic extracts were dried (Na₂SO₄) and the solvent was removed *in vacuo*. Purification of the residue by flash-chromatography (10 : 1 CHCl₃–MeOH) yielded **17** (58 mg, 55%): IR ν_{\max} (NaCl; cm⁻¹) 2759, 1787, 1740, 1210, 1090; δ_{H} (300 MHz, CDCl₃) 5.27 (1 H, t, *J* 7.2, 4-H), 4.97 (1 H, s, OCHHO), 4.69 (1 H, s, OCHHO), 4.61–4.59 (2 H, m, 1-H, 2-H), 2.82 (4 H, s, CH₂CH₂), 2.38 (2 H, dd, *J* 6.2, 14.2, 3-H', 5-H') and 1.99–1.89 (2 H, m, 3-H'', 5-H''); δ_{C} (100 MHz, CDCl₃) 168.6, 150.8, 94.5, 81.2, 78.1, 37.3 and 25.4; *m/z* (CI) 270 (M – H, 100); HRMS (M – H)⁺ calcd for C₁₁H₁₂NO₇, 270.0614; found, 270.0607.

(5αa,7β,8αa)-7-(4-nitrophenoxycarbonyloxy)-tetrahydrocyclopent[*f*]-1,3,5-trioxepane (18)

To a solution of **10** (15 mg, 0.094 mmol) and *N*-methylmorpholine (31 μL, 0.28 mmol) in dry THF (3 mL), *p*-nitrophenylchloroformate (57 mg, 0.28 mmol) was added and the resulting mixture was stirred at 23 °C. After 1 h, water was added, the solvent was removed under reduced pressure and the aqueous phase was extracted with CHCl₃. The organic extracts were dried (Na₂SO₄) and the solvent evaporated. The residue was purified by flash-chromatography (1 : 4 EtOAc–CHCl₃) to afford **18** (31 mg, 95%) as a pale yellow viscous oil: IR ν_{\max} (NaCl; cm⁻¹) 2831, 2598, 1766, 1529, 1350, 1116 and 859; δ_{H} (300 MHz, CDCl₃) 8.27 (2 H, d, *J* 8.7, ArH), 7.38 (2 H, d, *J* 8.7, ArH), 5.34–5.31 (1 H, m, 7-H), 5.19 (2 H, d, *J* 6.9, 2-H', 4-H'), 4.77 (2 H, d, *J* 6.9, 2-H'', 4-H''), 4.51–4.47 (2 H, m, 5a-H, 8a-H) and 2.38–2.26 (4 H, m, 6-H₂, 8-H₂); δ_{C} (75 MHz, CDCl₃) 155.3, 126.2, 125.3, 121.7, 115.6, 95.5, 81.2, 78.5 and 37.6; *m/z* (EI) 325 (M, 100).

(1β,2β,4β)-4-(4-Nitrophenoxycarbonyloxy)-1,2-(methylenedioxy)cyclopentane (19)

The title compound **19** was obtained from **11** as described for **18** in 81% yield. Flash-chromatography was performed using 1 : 1 EtOAc–Hex: IR ν_{\max} (NaCl; cm⁻¹) 2739, 1764, 1527, 1348 and 1204; δ_{H} (300 MHz, CDCl₃) 8.27 (2 H, d, *J* 5.1, ArH), 7.38 (2 H, d, *J* 5.1, ArH), 5.20–5.16 (2 H, m, OCH₂O), 4.83–4.81 (1 H, m, 4-H), 4.68 (2 H, d, *J* 5.7, 1-H, 2-H), 2.38 (2 H, d, *J* 14.7, 3-H', 5-H') and 2.11–2.02 (2 H, m, 3-H'', 5-H''); δ_{C} (100 MHz, CDCl₃)

155.4, 126.1, 125.2, 121.8, 115.5, 95.0, 80.7, 80.4 and 38.4; m/z (CI) 296 (M + H, 100); HRMS (M + H)⁺ calcd for C₁₃H₁₄NO₇, 296.0770; found, 296.0769.

(5α,7α,8α)-7-(4-Nitrophenoxycarbonyloxy)-tetrahydrocyclopenta[*f*]-1,3,5-trioxepane (20)

The title compound was obtained from **12** as described for **18** in 94% yield. Flash-chromatography was performed using 1 : 6 EtOAc–CHCl₃; IR ν_{\max} (NaCl; cm⁻¹) 2587, 1765, 1594, 1528, 1349 and 858; δ_{H} (300 MHz, CDCl₃) 8.25 (2 H, d, *J* 8.0, ArH), 7.39 (2 H, d, *J* 8.0, ArH), 5.20 (2 H, d, *J* 7.5, 2-H', 4-H'), 5.10–5.02 (1 H, m, 7-H), 4.75 (2 H, d, *J* 7.5, 2-H'', 4-H''), 4.29–4.24 (2 H, m, 5a-H, 8a-H), 2.51–2.41 (2 H, m, 6-H', 8-H') and 2.25–2.17 (2 H, m, 6-H'', 8-H''); δ_{C} (75 MHz, CDCl₃) 155.2, 126.2, 125.2, 121.7, 115.6, 94.6, 80.8, 76.6 and 36.9; m/z (CI) 324 (M – H, 100).

(1β,2β,4α)-4-(4-Nitrophenoxycarbonyloxy)-1,2-(ethylenedioxy)cyclopentane (21)

The title compound was obtained from **15** as described for **18** in 81% yield. Flash-chromatography was performed using 1 : 4 EtOAc–CHCl₃; IR ν_{\max} (NaCl; cm⁻¹) 2655, 1757, 1592, 1503, 1337, 852 and 754; δ_{H} (300 MHz, CDCl₃) 8.29 (2 H, d, *J* 7.3, ArH), 7.36 (2 H, d, *J* 7.3, ArH), 5.22–5.18 (1 H, m, 4-H), 3.86–3.84 (2 H, m, 1-H, 2-H), 3.78–3.63 (4 H, m, CH₂O), 2.38–2.24 (4 H, m, 3-H₂, 5-H₂); δ_{C} (100 MHz, CDCl₃) 161.8, 126.2, 125.3, 121.7, 115.6, 78.1, 74.3, 62.1 and 33.9; m/z (CI) 310 (M + H, 100).

(1β,2β,4β)-4-(4-Nitrophenoxycarbonyloxy)-1,2-(ethylenedioxy)cyclopentane (22)

The title compound was obtained from **16** as described for **18** in 95% yield. Flash-chromatography was performed using 1 : 4 EtOAc–CHCl₃; IR ν_{\max} (NaCl; cm⁻¹) 2588, 1725, 1594, 1222, 1109 and 773; δ_{H} (400 MHz, CDCl₃) 8.27 (2 H, d, *J* 7.0, ArH), 7.38 (2 H, d, *J* 7.0, ArH), 5.14–5.10 (1 H, m, 4-H), 3.99 (2 H, t, *J* 4.6, 1-H, 2-H), 3.91–3.86 (2 H, m, CH₂O), 3.64–3.59 (2 H, m, CH₂O) and 2.31–2.18 (4 H, m, 3-H₂, 5-H₂); δ_{C} (100 MHz, CDCl₃) 162.5, 126.1, 125.2, 121.7, 115.5, 81.4, 74.3, 62.3 and 32.5; m/z (CI) 310 (M + H, 100).

(1'S,2'R)-{1'-Benzyl-2'-hydroxy-3'-[isobutyl(4-methoxybenzenesulfonyl)amino]propyl} carbamic acid (1β,2β,4β)-1,2-(methylenedioxy)cyclopent-4-yl ester (2)

A solution of **24** (25 mg, 0.05 mmol) in 30% trifluoroacetic acid in CH₂Cl₂ (4 mL) was stirred at 23 °C for 40 min and then the solvent was removed under reduced pressure. The residue was dissolved in THF (3 mL), a solution of **19** (18 mg, 0.059 mmol) in THF (1 mL) and diisopropylethylamine (100 μL, 0.6 mmol) were added. After 24 h the organic phase was diluted with CHCl₃, washed with water, dried (Na₂SO₄), and evaporated. The residue was purified by flash-chromatography eluting with a 1 : 1 mixture of EtOAc and hexanes to afford **2** (20 mg, 74%) as a white solid: $[\alpha]_{\text{D}}^{20} +4.5$ (*c* 1.2 in CH₂Cl₂), mp 68 °C (from EtOAc–Hex); IR ν_{\max} (NaCl; cm⁻¹) 3129, 2801, 2660, 1711, 1597, 1497, 1155 and 761; δ_{H} (300 MHz, CDCl₃) 7.71 (2 H, d, *J* 8.8, ArH), 7.32–7.19 (5 H, m, ArH), 6.98 (2 H, d, *J* 8.8, ArH), 5.01 (1 H, s, OCHHO), 4.92 (1 H, br. s, NH), 4.80 (2 H, m, 4-H, OCHHO), 4.57 (2 H,

d, *J* 5.4, 1-H, 2-H), 3.87 (3 H, s, OCH₃), 3.79 (2 H, m, CHN, CHOH), 3.10–2.76 (6 H, m, CH₂N, CH₂Ph), 2.11–1.80 [5 H, m, 3-H₂, 5-H₂, CH(CH₃)₂], 0.90 (3 H, d, *J* 6.6, CHCH₃) and 0.86 (3 H, d, *J* 6.6, CHCH₃); δ_{C} (75 MHz, CDCl₃) 162.9, 155.3, 137.5, 129.9, 129.6, 129.3, 128.5, 126.4, 114.3, 94.7, 80.5, 74.2, 72.3, 58.8, 55.6, 54.9, 53.8, 38.5, 35.4, 27.3, 20.2 and 19.9; m/z (ES) 563 (M + H, 100); HRMS (M + H)⁺ calcd For C₂₈H₃₉N₂O₈S, 563.2427; found, 563.2406.

(1'S,2'R)-{1'-Benzyl-2'-hydroxy-3'-[isobutyl(4-methoxybenzenesulfonyl)amino]propyl} carbamic acid (1β,2β,4α)-1,2-(methylenedioxy)cyclopent-4-yl ester (26)

A solution of **24** (40 mg, 0.079 mmol) in 30% trifluoroacetic acid in CH₂Cl₂ (6 mL) was stirred at 23 °C for 40 min and then the solvent was removed under reduced pressure. The residue was dissolved in CH₂Cl₂ (4 mL), a solution of **17** (23 mg, 0.1 mmol) in CH₂Cl₂ (2 mL) and diisopropylethylamine (140 μL, 0.8 mmol) were added. After 2 h the organic phase was washed with water, dried (Na₂SO₄) and evaporated. The residue was purified by flash-chromatography (1 : 1 EtOAc–Hex) to afford **26** (34 mg, 76%) as a white foam: $[\alpha]_{\text{D}}^{20} +3.6$ (*c* 1.3 in CH₂Cl₂); IR ν_{\max} (NaCl; cm⁻¹) 3216, 2801, 2670, 1712, 1597, 1497, 1154 and 755; δ_{H} (300 MHz, CDCl₃) 7.70 (2 H, d, *J* 8.7, ArH), 7.32–7.21 (5 H, m, ArH), 7.00 (2 H, d, *J* 8.7, ArH), 5.06 (1 H, t, *J* 7.0, 4-H), 4.93 (1 H, s, OCHHO), 4.76 (1 H, d, *J* 8.4, NH), 4.71 (1 H, s, OCHHO), 4.52 (2 H, m, 1-H, 2-H), 3.87 (3 H, s, OCH₃), 3.84 (2 H, m, CHN, CHOH), 3.11 (1 H, dd, *J* 8.0, 14.8, CHHN), 3.04–2.91 (4 H, m, CHHN, CH₂N, CHHPh), 2.78 (1 H, dd, *J* 6.7, 13.1, CHHPh), 2.17–2.10 (2 H, m, 3-H', 5-H'), 1.86–1.58 [3 H, m, 3-H'', 5-H'', CH(CH₃)₂], 0.91 (3 H, d, *J* 6.6, CHCH₃) and 0.87 (3 H, d, *J* 6.9, CHCH₃); δ_{C} (75 MHz, CDCl₃) 162.9, 155.8, 137.6, 129.9, 129.7, 129.4, 128.4, 126.5, 114.3, 94.3, 78.5, 74.5, 72.6, 58.8, 55.6, 54.9, 53.7, 37.8, 35.3, 27.3, 20.2 and 19.9; m/z (ES) 585 (M + Na, 100); HRMS (M + Na)⁺ calcd for C₂₈H₃₈N₂NaO₈S, 585.2247; found, 585.2228.

(1S,2R)-{1'-Benzyl-2'-hydroxy-3'-[isobutyl(4-methoxybenzenesulfonyl)amino]propyl} carbamic acid (5α,7β,8α)-tetrahydrocyclopenta[*f*]-1,3,5-trioxepan-7-yl ester (27)

The title compound was obtained from **24** and **18** as described for **2** in 43% yield. Flash-chromatography was performed with 1 : 4 EtOAc–CHCl₃; $[\alpha]_{\text{D}}^{20} +5.2$ (*c* 1.7 in CH₂Cl₂); IR ν_{\max} (NaCl; cm⁻¹) 3118, 2825, 2656, 1712, 1596, 1012 and 771; δ_{H} (300 MHz, CDCl₃) 7.70 (2 H, d, *J* 9.0, ArH), 7.32–7.21 (5 H, m, ArH), 6.98 (2 H, d, *J* 9.0, ArH), 5.15 (2 H, d, *J* 7.2, 2-H', 4-H'), 5.05 (1 H, br. s, NH), 4.76 (1 H, d, *J* 8.4, 7-H), 4.68 (2 H, d, *J* 7.2, 2-H'', 4-H''), 4.32–4.23 (2 H, m, 5a-H, 8a-H), 3.87 (3 H, s, OCH₃), 3.83–3.80 (2 H, m, CHN, CHOH), 3.10 (1 H, dd, *J* 8.4, 15.3, CHHN), 3.04–2.88 (4 H, m, CHHN, CH₂N, CHHPh), 2.78 (1 H, dd, *J* 6.9, 13.5, CHHPh), 2.09–1.94 (4 H, m, 6-H₂, 8-H₂), 1.86–1.77 [1 H, m, CH(CH₃)₂], 0.91 (3 H, d, *J* 6.9, CHCH₃) and 0.87 (3 H, d, *J* 6.3, CHCH₃); δ_{C} (75 MHz, CDCl₃) 163.0, 155.7, 137.6, 129.8, 129.7, 129.4, 128.4, 126.5, 114.3, 95.4, 81.5, 73.6, 72.7, 58.8, 55.7, 54.9, 53.7, 37.8, 35.4, 27.3, 20.2 and 19.9; m/z (ES) 615 (M + Na, 100); HRMS (M + Na)⁺ calcd for C₂₉H₄₀N₂NaO₉S, 615.2353; found, 615.2361.

(1'S,2'R)-{1'-Benzyl-2'-hydroxy-3'-[isobutyl(4-methoxybenzenesulfonyl)amino]propyl} carbamic acid (5aa,7a,8aa)-tetrahydrocyclopent[*f*]-1,3,5-trioxepan-7-yl ester (28)

The title compound was obtained from **24** and **20** as described for **2** in 42% yield. Flash-chromatography was performed with 1 : 1 EtOAc–Hex: $[\alpha]_{\text{D}}^{20} +7.3$ (*c* 1.7 in CH₂Cl₂); IR ν_{max} (NaCl; cm⁻¹) 3117, 2801, 2707, 1711, 1596, 1260 and 1153; δ_{H} (300 MHz, CDCl₃) 7.70 (2 H, d, *J* 8.7, ArH), 7.31–7.21 (5 H, m, ArH), 6.97 (2 H, d, *J* 8.7, ArH), 5.14 (2 H, d, *J* 6.9, 2-H', 4-H'), 4.91 (1 H, d, *J* 7.8, NH), 4.83–4.78 (1 H, m, 7-H), 4.68 (2 H, d, *J* 6.9, 2-H'', 4-H''), 4.15–4.10 (2 H, m, 5a-H, 8a-H), 3.87 (3 H, s, OCH₃), 3.81–3.83 (2 H, m, CHN, CHOH), 3.12–2.85 (5 H, m, 2 × CH₂N, CHHPh), 2.77 (1 H, dd, *J* 6.9, 13.5, CHHPh), 2.34–2.21 (2 H, m, 6-H', 8-H'), 1.94–1.76 [3 H, m, 6-H'', 8-H'', CH(CH₃)₂], 0.90 (3 H, d, *J* 6.6, CHCH₃) and 0.86 (3 H, d, *J* 6.6, CHCH₃); δ_{C} (100 MHz, CDCl₃) 162.9, 156.1, 137.5, 129.8, 129.5, 129.4, 128.4, 126.4, 114.3, 94.8, 81.0, 72.3, 71.3, 58.6, 55.6, 55.0, 53.6, 37.1, 35.5, 27.1, 20.1 and 19.8; *m/z* (ES) 615 (M + Na, 100); HRMS (M + Na)⁺ calcd for C₂₉H₄₀N₂NaO₉S, 615.2353; found, 615.2349.

(1'S,2'R)-{1'-Benzyl-2'-hydroxy-3'-[isobutyl(4-methoxybenzenesulfonyl)amino]propyl} carbamic acid (1β,2β,4β)-1,2-(ethylenedioxy)cyclopent-4-yl ester (3)

The title compound was obtained from **24** and **22** as described for **2** in 40% yield. Flash-chromatography was performed with 1 : 1 EtOAc–Hex: $[\alpha]_{\text{D}}^{20} +6.9$ (*c* 0.7 in CH₂Cl₂); IR ν_{max} (NaCl; cm⁻¹) 3120, 2788, 2656, 2542, 1712, 1596, 1259, 1154 and 755; δ_{H} (500 MHz, CDCl₃) 7.70 (2 H, d, *J* 9.0, ArH), 7.31–7.22 (5 H, m, ArH), 6.97 (2 H, d, *J* 9.0, ArH), 4.90–4.86 (2 H, m, NH, 4-H), 3.87 (3 H, s, OCH₃), 3.85–3.79 (7 H, m, 2 × CH₂O, 1-H, 2-H, OH), 3.57–3.54 (2 H, m, CHN, CHOH), 3.11 (1 H, dd, *J* 8.2, 14.7, CHHN), 3.03–2.88 (4 H, m, CHHN, CH₂N, CHHPh), 2.78 (1 H, dd, *J* 6.7, 13.2, CHHPh), 2.17–2.08 (2 H, m, 3-H', 5-H'), 1.98–1.95 (2 H, m, 3-H'', 5-H''), 1.90 [1 H, dt, *J* 5.2, 15.0, CH(CH₃)₂], 0.91 (3 H, d, *J* 6.5, CHCH₃) and 0.86 (3 H, d, *J* 6.5, CHCH₃); δ_{C} (75 MHz, CDCl₃) 163.0, 156.2, 137.6, 129.8, 129.6, 129.5, 128.5, 126.5, 114.3, 74.5, 73.2, 72.5, 71.8, 62.5, 62.3, 58.8, 55.6, 55.0, 53.8, 35.5, 33.8, 33.5, 27.3, 20.2 and 19.9; *m/z* (ES) 599 (M + Na, 100); HRMS (M + Na)⁺ calcd for C₂₉H₄₀N₂NaO₈S, 599.2403; found, 599.2394.

(1'S,2'R)-{1'-Benzyl-2'-hydroxy-3'-[isobutyl(4-methoxybenzenesulfonyl)amino]propyl} carbamic acid (1β,2β,4α)-1,2-(ethylenedioxy)cyclopent-4-yl ester (29)

The title compound was obtained from **24** and **21** as described for **2** in 40% yield. Flash-chromatography was performed with 1 : 1 EtOAc–Hex: $[\alpha]_{\text{D}}^{20} +8.2$ (*c* 1.0 in CH₂Cl₂); IR ν_{max} (NaCl; cm⁻¹) 3121, 2706, 1711, 1596, 1260, 1154 and 757; δ_{H} (500 MHz, CDCl₃) 7.70 (2 H, d, *J* 8.7, ArH), 7.31–7.28 (2 H, m, ArH), 7.24–7.22 (3 H, m, ArH), 6.98 (2 H, d, *J* 8.7, ArH), 5.09 (1 H, br. s, NH), 4.74 (1 H, d, *J* 8.0, 4-H), 4.06–4.01 (2 H, m, 1-H, 2-H), 3.87 (3 H, s, OCH₃), 3.82–3.81 (2 H, m, CH₂O), 3.75–3.71 (2 H, m, CH₂O), 3.55–3.51 (2 H, m, CHN, CHOH), 3.10 (1 H, dd, *J* 15.0, 8.5, CHHN), 3.03–2.86 (4 H, m, CHHN, CH₂N, CHHPh), 2.78 (1 H, dd, *J* 13.5, 6.5, CHHPh), 2.32–2.23 (2 H, m, 3-H', 5-H'), 1.81 (1 H, q, *J* = 6.5, 3-H''), 1.79–1.68 (1 H, m, 5-H''), 1.62–1.53 [1

H, m, CH(CH₃)₂], 0.91 (3 H, d, *J* 6.6, CHCH₃) and 0.86 (3 H, d, *J* 6.6, CHCH₃); δ_{C} (75 MHz, CDCl₃) 163.1, 156.1, 137.6, 129.8, 129.6, 129.5, 128.5, 126.6, 114.4, 74.6, 73.2, 72.7, 62.2, 58.8, 55.7, 54.9, 53.8, 35.4, 34.3, 34.2, 27.3, 20.2 and 19.9; *m/z* (ES) 599 (M + Na, 100); HRMS (M + H)⁺ calcd for C₂₉H₄₀N₂NaO₈S, 599.2403; found, 599.2421.

(1'S,2'R)-{1'-Benzyl-2'-hydroxy-3'-[isobutyl(4-(hydroxymethyl)benzenesulfonyl)amino]propyl} carbamic acid (1β,2β,4β)-1,2-(methylenedioxy)cyclopent-4-yl ester (30)

To a solution of **25**⁸ (40 mg, 0.1 mmol) and diisopropylethylamine (150 μL, 0.9 mmol) in THF (3 mL), a solution of **17** (30 mg, 0.11 mmol) was added and the resulting mixture was stirred at 23 °C. After 48 h, the organic phase was diluted with CHCl₃, washed with water, dried (Na₂SO₄) and evaporated. The residue was purified by flash-chromatography (2 : 1 EtOAc–Hex) to afford **30** (35 mg, 63%) as an amorphous solid: $[\alpha]_{\text{D}}^{20} +7.8$ (*c* 1.3 in CHCl₃); IR ν_{max} (NaCl; cm⁻¹) 3042, 2996, 2707, 1710, 1530, 1334, 1156 and 755; δ_{H} (400 MHz, CDCl₃) 7.77 (2 H, d, *J* 8.1, ArH), 7.52 (2 H, d, *J* 8.1, ArH), 7.32–7.21 (5 H, m, ArH), 5.00 (1 H, s, NH), 4.92 (1 H, m, 4-H), 4.82–4.80 (4 H, m, OCH₂O, CH₂OH), 4.58–4.57 (2 H, m, 1-H, 2-H), 3.81–3.79 (2 H, m, CHN, CHOH), 3.11–2.83 (6 H, m, 2 × CH₂N, CH₂Ph), 2.10–1.82 [5 H, m, 3-H₂, 5-H₂, CH(CH₃)₂], 0.91 (3 H, d, *J* 6.6, CHCH₃) and 0.83 (3 H, d, *J* 6.6, CHCH₃); δ_{C} (100 MHz, CDCl₃) 156.2, 146.2, 137.5, 137.1, 129.5, 128.5, 127.5, 127.1, 126.5, 94.6, 80.5, 75.8, 72.2, 64.0, 58.5, 55.1, 53.5, 38.4, 35.4, 27.1, 20.0 and 19.8; *m/z* (ES) 585 (M + Na, 100); HRMS (M + Na)⁺ calcd for C₂₈H₃₈N₂NaO₈S, 585.2247; found, 585.2246.

X-Ray crystallography. The HIV-1 protease construct with the substitutions Q7K, L33I, L63I, C67A, and C95A to optimize protein stability,²⁰ was expressed and purified as described.²¹ Crystals were grown by the hanging drop vapor diffusion method using a 1 : 15 molar ratio of protease at 2.0 mg mL⁻¹ and the inhibitor dissolved in dimethylsulfoxide. The reservoir contained 0.1 M sodium acetate buffer (pH = 4.2) and 1.5 M NaCl. Crystals were transferred into a cryoprotectant solution containing the reservoir solution and 20–30% (v/v) glycerol, mounted on a nylon loop and flash-frozen in liquid nitrogen. X-ray diffraction data were collected on the SER-CAT beamline of the Advanced Photon Source, Argonne National Laboratory. Diffraction data were processed using HKL2000²² resulting in a *R*_{merge} value of 7.0% (41.8%) for 90 315 unique reflections between 50 and 1.07 Å resolution with a completeness of 88.1% (51.3%), where the values in parentheses are for the final highest resolution shell. Data were reduced in space group *P*2₁2₁2 with unit cell dimensions of *a* = 58.00 Å, *b* = 86.34 Å and *c* = 45.83 Å with one dimer in the asymmetric unit. The structure was solved by molecular replacement using the CPP4i suite of programs,^{23,24} with the structure of the D30N mutant of HIV protease in complex with GRL-98065 (2QCI)¹⁹ as the starting model. The structure was refined using SHELX97²⁵ and refitted manually using the molecular graphics programs O²⁶ and COOT.²⁷ Alternate conformations were modeled for the protease residues when obvious in the electron density maps. Anisotropic atomic displacement parameters (*B*-factors) were refined for all atoms including solvent molecules. Hydrogen atoms were added at the final stages of the refinement. The identity of ions and other solvent molecules from the crystallization conditions was

deduced from the shape and peak height of the $2F_o - F_c$ and $F_o - F_c$ electron density, the hydrogen bond interactions and interatomic distances. The solvent structure was refined with one sodium ion, three chloride ions, and 203 water molecules including partial occupancy sites. The final R_{work} was 15.2% and RB_{free} was 17.7% for all data between 10 and 1.07 Å resolution. The rmsd values from ideal bonds and angle distances were 0.015 Å and 0.034 Å, respectively. The average B -factor was 13.1 and 18.2 Å² for protease main chain and side chain atoms, respectively, 12.5 Å² for inhibitor atoms and 24.0 Å² for solvent atoms. The X-ray crystal structure of the inhibitor **3** complex with the HIV-1 protease has been deposited in the Protein Databank (PDB)²⁸ with an access code of 3DKJ.

Acknowledgements

The research was supported by grants from the National Institutes of Health (GM53386, AKG, and GM62920, IW). This work was also supported by the Intramural Research Program of the Center for Cancer Research, National Cancer Institute, National Institutes of Health and in part by a Grant-in-aid for Scientific Research (Priority Areas) from the Ministry of Education, Culture, Sports, Science, and Technology of Japan (Monbu Kagakusho), a Grant for Promotion of AIDS Research from the Ministry of Health, Welfare, and Labor of Japan (Kosei Rohdoshō: H15-AIDS-001), and a Grant to the Cooperative Research Project on Clinical and Epidemiological Studies of Emerging and Re-emerging Infectious Diseases (Renkei Jigyō: No. 78, Kumamoto University) of Monbu-Kagakusho.

Notes and references

- (a) N. A. Roberts, J. A. Martin, D. Kinchington, A. V. Broadhurst, J. C. Craig, I. B. Duncan, S. A. Galpin, B. K. Handa, J. Kay and A. Krohn, *Science*, 1990, **248**, 358; (b) T. D. Meek, D. M. Lambert, G. B. Dreyer, T. J. Carr, T. A. Tomaszek, M. L. Moore, J. E. Strickler, C. Debouck, L. J. Hyland, T. J. Matthews, B. W. Metcalf and S. R. Petteway, *Nature*, 1990, **343**, 90; (c) T. J. McQuade, A. G. Tomasselli, L. Liu, V. Karacostas, B. Moss, T. K. Sawyer, R. L. Henrikson and W. G. Tarpley, *Science*, 1990, **247**, 454.
- (a) C. Flexner, *N. Engl. J. Med.*, 1998, **338**, 1281; (b) T. Cihlar and N. Bischofberger, *Annu. Rep. Med. Chem.*, 2000, **35**, 177.
- (a) M. A. Wainberg and G. Friedland, *JAMA, J. Am. Med. Assoc.*, 1998, **279**, 1977; (b) S. Grabar, C. Pradier, E. Le Corfec, R. Lancar, C. Allavena, M. Bentata, P. Berleau, C. Dupont, P. Fabbro-Peray, I. Poizot-Martin and D. Costagliola, *AIDS*, 2000, **14**, 141; (c) K. Hertogs, S. Bloor, S. D. Kemp, C. Van den Eynde, T. M. Alcorn, R. Pauwels, M. Van Houtte, S. Staszewski, V. Miller and B. A. Larder, *AIDS*, 2000, **14**, 1203.
- On June 23, 2006, the FDA approved a new HIV treatment for patients who do not respond to existing drugs. <http://www.fda.gov/bbs/topics/NEWS/2006/NEW01395.html>.
- (a) D. L. N. G. Surleraux, A. Tahri, W. G. Verschuere, G. M. E. Pille, H. A. de Kock, T. H. M. Jonckers, A. Peeters, S. De Meyer, H. Azijn, R. Pauwels, M.-P. de Bethune, N. M. King, M. Prabu-Jeyabalan, C. A. Schiffer and P. B. T. P. Wigerinck, *J. Med. Chem.*, 2005, **48**, 1813; (b) Y. Koh, H. Nakata, K. Maeda, H. Ogata, G. Bilcer, T. Devasamudram, J. F. Kincaid, P. Boross, Y.-F. Wang, Y. Tie, P. Volarath, L. Gaddis, R. W. Harrison, I. T. Weber, A. K. Ghosh and H. Mitsuya, *Antimicrob. Agents Chemother.*, 2003, **47**, 3123; (c) A. K. Ghosh, E. Pretzer, H. Cho, K. A. Hussain and N. Duzgunes, *Antiviral Res.*, 2002, **54**, 29.
- (a) A. K. Ghosh, J. F. Kincaid, W. Cho, D. E. Walters, K. Krishnan, K. A. Hussain, Y. Koo, H. Cho, C. Rudall, L. Holland and J. Buthod, *Bioorg. Med. Chem. Lett.*, 1998, **8**, 687; (b) K. Yoshimura, R. Kato, M. F. Kavlick, A. Nguyen, V. Maroun, K. Maeda, K. A. Hussain, A. K. Ghosh, S. V. Gulnik, J. W. Erickson and H. Mitsuya, *J. Virol.*, 2002, **76**, 1349.
- (a) A. K. Ghosh, J. F. Kincaid, W. Cho, D. E. Walters, K. Krishnan, K. A. Hussain, Y. Koo, H. Cho, C. Rudall, L. Holland and J. Buthod, *Bioorg. Med. Chem. Lett.*, 1998, **8**, 687; (b) K. Yoshimura, R. Kato, M. F. Kavlick, A. Nguyen, V. Maroun, K. Maeda, K. A. Hussain, A. K. Ghosh, S. V. Gulnik, J. W. Erickson and H. Mitsuya, *J. Virol.*, 2002, **76**, 1349.
- A. K. Ghosh, P. R. Sridhar, S. Leshchenko, A. K. Hussain, J. Li, A. Y. Kovalevsky, D. E. Walters, J. E. Wedekind, V. Grum-Tokars, D. Das, Y. Koh, K. Maeda, H. Gatanaga, I. T. Weber and H. Mitsuya, *J. Med. Chem.*, 2006, **49**, 5252.
- P. Ashkenazi, J. Kalo, A. Rüttimann and D. Ginsburgh, *Tetrahedron*, 1978, 2161.
- G. Godjoian, V. R. Wang, A. M. Ayala, R. V. Martínez, R. Martínez-Bernhardt and C. G. Gutiérrez, *Tetrahedron Lett.*, 1996, **37**, 433.
- A. K. Ghosh, T. T. Duong, S. P. McKee and W. J. Thompson, *Tetrahedron Lett.*, 1992, **33**, 2781.
- A. K. Ghosh and S. Fidanze, *J. Org. Chem.*, 1998, **63**, 6146.
- M. V. Toth and G. R. Marshall, *Int. J. Pept. Protein Res.*, 1990, **36**, 544.
- C. F. Perno, R. Yarchoan, D. A. Cooney, N. R. Hartman, D. S. A. Webb, Z. Hao, H. Mitsuya, D. G. Johns and S. Broder, *J. Exp. Med.*, 1989, **169**, 933.
- Y. Tie, P. I. Boross, Y. F. Wang, L. Gaddis, F. Liu, X. Chen, J. Tozser, R. W. Harrison and I. T. Weber, *FEBS J.*, 2005, **272**, 5265.
- A. Gustchina, C. Sansom, M. Prevost, J. Richelle, S. Wodak, A. Wlodawer and I. Weber, *Protein Eng.*, 1994, **7**, 309.
- S. Panigrahi and G. Desiraju, *Proteins: Struct., Funct., Bioinf.*, 2007, **67**, 128.
- T. Steiner, *Biophys. Chem.*, 2002, **95**, 195.
- Y. F. Wang, Y. Tie, P. I. Boross, J. Tozser, A. K. Ghosh, R. W. Harrison and I. T. Weber, *J. Med. Chem.*, 2007, **50**, 4509.
- J. M. Louis, G. M. Clore and A. M. Gronenborn, *Nat. Struct. Biol.*, 1999, **6**, 868.
- B. Mahalingam, J. M. Louis, J. Hung, R. W. Harrison and I. T. Weber, *Proteins: Struct., Funct., Genet.*, 2001, **43**, 455–464.
- Z. Otwinowski and W. Minor, *Methods Enzymol.*, 1997, **276**, 307.
- Collaborative Computational Project, Number 4. The CCP4 Suite: Programs for Protein Crystallography, *Acta Crystallogr.*, 1994, **D50**, 760.
- E. Potterton, P. Briggs, M. Turkenburg and E. Dodson, *Acta Crystallogr.*, 2003, **D59**, 1131.
- G. M. Sheldrick and T. R. Schneider, *Methods Enzymol.*, 1997, **277**, 319.
- T. A. Jones, J. Y. Zou, S. W. Cowan and M. Kjeldgaard, *Acta Crystallogr.*, 1991, **A47**, 110.
- P. Emsley and K. Cowtan, *Acta Crystallogr.*, 2004, **D60**, 2126.
- H. M. Berman, J. Westbrook, Z. Feng, G. Gilliland, T. N. Bhat, H. Weissig, I. N. Shindyalov and P. E. Bourne, *Nucleic Acids Res.*, 2000, **28**, 235.

Flexible Cyclic Ethers/Polyethers as Novel P2-Ligands for HIV-1 Protease Inhibitors: Design, Synthesis, Biological Evaluation, and Protein–Ligand X-ray Studies[†]

Arun K. Ghosh,^{*,‡} Sandra Gemma,[‡] Abigail Baldrige,[‡] Yuan-Fang Wang,[§] Andrey Yu. Kovalevsky,[§] Yashiro Koh,^{||} Irene T. Weber,[§] and Hiroaki Mitsuya^{||,⊥}

Departments of Chemistry and Medicinal Chemistry, Purdue University, 560 Oval Drive, West Lafayette, Indiana 47907, Department of Biology, Molecular Basis of Disease, Georgia State University, Atlanta, Georgia 30303, Kumamoto University School of Medicine, Kumamoto 860-8556, Japan, Department of Hematology and Infectious Diseases, Experimental Retrovirology Section, HIV and AIDS Malignancy Branch, National Cancer Institute, Bethesda, Maryland 20892

Received April 21, 2008

We report the design, synthesis, and biological evaluation of a series of novel HIV-1 protease inhibitors. The inhibitors incorporate stereochemically defined flexible cyclic ethers/polyethers as high affinity P2-ligands. Inhibitors containing small ring 1,3-dioxacycloalkanes have shown potent enzyme inhibitory and antiviral activity. Inhibitors **3d** and **3h** are the most active inhibitors. Inhibitor **3d** maintains excellent potency against a variety of multi-PI-resistant clinical strains. Our structure–activity studies indicate that the ring size, stereochemistry, and position of oxygens are important for the observed activity. Optically active synthesis of 1,3-dioxepan-5-ol along with the syntheses of various cyclic ether and polyether ligands have been described. A protein–ligand X-ray crystal structure of **3d**-bound HIV-1 protease was determined. The structure revealed that the P2-ligand makes extensive interactions including hydrogen bonding with the protease backbone in the S2-site. In addition, the P2-ligand in **3d** forms a unique water-mediated interaction with the NH of Gly-48.

Introduction

The introduction of protease inhibitors (PIs) into highly active antiretroviral therapy (HAART), a combination therapy based on coadministration of PIs with reverse-transcriptase inhibitors, marked the beginning of a new era in HIV/AIDS chemotherapy. HAART treatment regimens have led to a significant decline in the number of deaths due to HIV infection in the developed world.¹ Unfortunately, there are a number of factors that severely limit current HAART treatment regimens. High frequency of dosing, heavy pill burden, and issues of tolerability and toxicity can lead to poor adherence to treatment.² The need for more potent, less toxic drug regimens is quite apparent.

It is the rapid emergence of drug resistance, however, that is proving to be the most formidable problem. Mutations causing drug resistance are thought to occur spontaneously, through the recombination of mixed viral populations, and also due to drug pressure, particularly when administered at substandard doses.^{3–6} A growing number of patients are developing multidrug-resistant HIV-1 variants.^{7,8} There is ample evidence that these viral strains can be transmitted. Thus, the development of antiretroviral agents able to maintain potency against resistant HIV strains has become an urgent priority.

Darunavir (TMC-114, **1**, Figure 1) is a new nonpeptidic PI recently approved by the FDA for the treatment of antiretroviral therapy-experienced patients.⁹ Inhibitor **1**, and its related analogue **2**, are exceedingly active against both wild-type and multidrug resistant HIV strains. Both PIs demonstrated potent

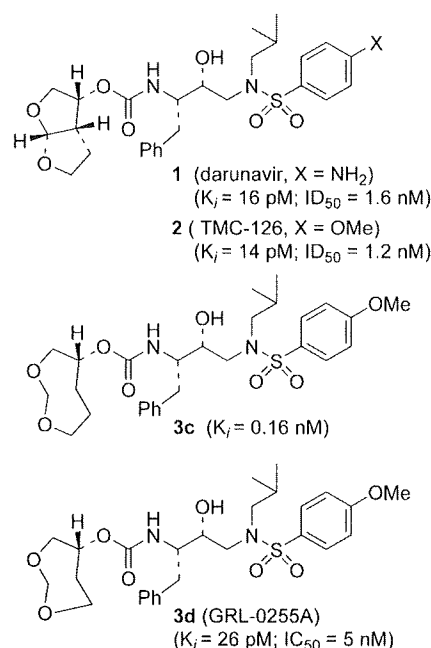


Figure 1. Structure of inhibitors **1**, **2**, and **3c,d**.

in vitro activity against viral isolates resistant to currently licensed PIs.^{10–12} Our structure-based design strategies for these PIs are based on the presumption that maximizing active site interactions with the inhibitor, particularly hydrogen bonding with the protein backbone, would give rise to potent inhibitors retaining activity against mutant strains.^{13,14} Indeed, side chain amino acid mutations cannot easily disrupt inhibitor–backbone interactions because the active site backbone conformation of mutant proteases is only minimally distorted compared to the wild-type HIV-1 protease.^{15–17} In this context, the fused bis-tetrahydrofuran (bis-THF) urethane of compounds **1** and **2** was demonstrated to be a privileged P2-ligand, being able to engage

[†] The PDB accession code for **3d**-bound HIV-1 protease X-ray structure is 3DJK.

^{*} To whom correspondence should be addressed. Phone: (765)-494-5323. Fax: (765)-496-1612. E-mail: akghosh@purdue.edu.

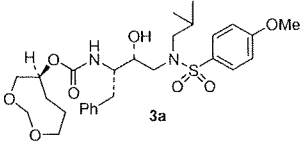
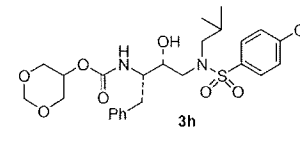
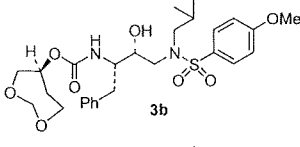
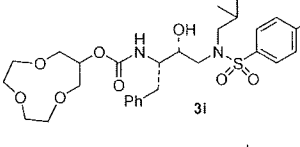
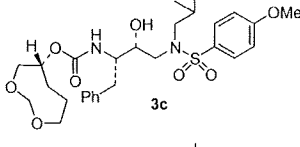
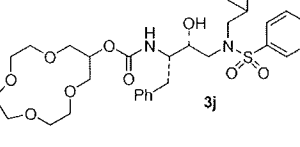
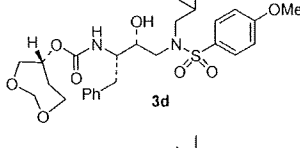
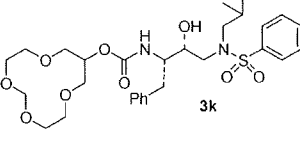
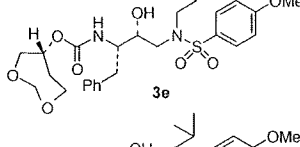
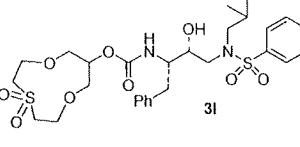
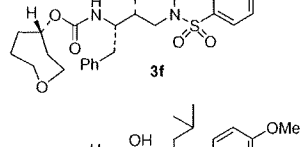
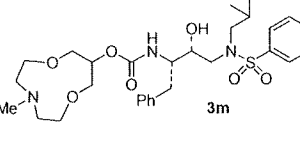
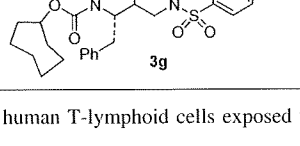
[‡] Departments of Chemistry and Medicinal Chemistry, Purdue University.

[§] Department of Biology, Molecular Basis of Disease, Georgia State University.

^{||} Kumamoto University School of Medicine.

[⊥] HIV and AIDS Malignancy Branch, National Cancer Institute.

Table 1. Enzyme Inhibitory and Antiviral Activity of Inhibitors 3a–m

entry	inhibitor	K_i (nM)	IC_{50} (nM) ^a	entry	inhibitor	K_i (nM)	IC_{50} (nM) ^a
1		0.15 ± 0.019	nd ^b	8		0.041 ± 0.002	3.4 ± 0.7
2		0.16 ± 0.04	30 ± 1	9		16 ± 2.2	nd
3		0.16 ± 0.011	nd	10		3.3 ± 1.9	nd
4		0.026 ± 0.012	4.9 ± 0.3	11		6.3 ± 0.57	>1000
5		0.81 ± 0.12	nd	12		1.9 ± 0.2	>1000
6		0.74 ± 0.15	nd	13		19 ± 0.76	>1000
7		27 ± 0.81	nd	SQV ^c	-	-	16 ± 3
				APV ^d	-	-	27 ± 6

^a MT-2 human T-lymphoid cells exposed to HIV-1_{LAI}. ^b nd = not determined. ^c SQV = saquinavir. ^d APV = amprenavir.

in a number of hydrogen bonding interactions with the backbone atoms of amino acids at the protease S2-site.

We are continuing our efforts toward the development of novel PIs characterized by a high activity against both wild-type HIV-1 and resistant strains. We further speculated that an inhibitor interacting strongly with the protein backbone, while being able to accommodate amino acid side chain variations by means of repacking with a flexible ring, would maintain significant affinity against both wild-type and mutant enzymes. With this goal in mind, we designed a series of PIs based on the (*R*)-(hydroxyethylamino)sulfonamide isostere and bearing flexible cyclic ethers and polyethers as P2-ligands (inhibitors 3a–m, Table 1). Starting from compound 3c, incorporating a (1*R*)-3,5-dioxacyclooctan-1-yl urethane, which can be considered as the flexible counterpart of the bis-THF moiety, we designed a series of structural variants of this inhibitor. These inhibitors contain polyether-based P2-ligands ranging from 6- to 13-membered rings coupled to a *p*-methoxyphenylsulfonamide as the P2'-ligand. Herein we report the structure-based design, synthesis, and preliminary biological evaluation of inhibitors 3a–m. Among these inhibitors, 3d (Figure 1) is the most potent, with an impressive enzyme inhibitory and antiviral activity (K_i = 26 pM, IC_{50} = 4.9 nM). Furthermore, a protein–ligand X-ray structure of 3d-bound HIV-1 protease has

revealed important molecular insight regarding ligand-binding site interactions.

Chemistry. The syntheses of seven- and eight-membered 1,3-dioxacycloalkanes 8a–d for the corresponding inhibitors 3a–d are shown in Scheme 1. Protected diol 6a was prepared by a two-step procedure starting from (*S*)-hydroxyglutaric acid 4, obtained by following a known protocol.¹⁸ The hydroxyl group of 4 was protected as a *tert*-butyldiphenylsilyl ether 5 in quantitative yield. LiBH₄ reduction of both ester groups afforded 6a in good yield.¹⁹

Compounds 6a and 6b²⁰ were converted to cyclic derivatives by exposure to paraformaldehyde and BF₃·OEt₂²¹ to afford cyclic ethers 7a and 7b in 51% and 82% yield, respectively. Deprotection of compounds 7a to 8a was carried out by using *n*-Bu₄N⁺F⁻ in THF. Benzylether of 7b was removed by a catalytic hydrogenation over 10% Pd–C to furnish 8b. Mitsunobu inversion of the secondary hydroxyl groups of 8a,b was accomplished by using *p*-nitrobenzoic acid, triphenylphosphine, and diisopropylazodicarboxylate in benzene at 23 °C. Saponification of the resulting esters provided 8c and 8d.

For the synthesis of compounds 8e and 8f, which represent the monooxygenated analogues of 8d, a synthetic strategy based on a ring-closing metathesis reaction as the key step was planned (Schemes 2 and 3). Accordingly, secondary alcohol 9²² (Scheme